2006

Differences of DNA-Transcription Factor Interactions Following Chromium Exposure

Kathryn Louise Mintz
The University of Montana

DIFFERENCES OF DNA-TRANSCRIPTION FACTOR INTERACTIONS FOLLOWING CHROMIUM EXPOSURE

By

Kathryn Louise Mintz

B.S. Chemistry, The Georgia Institute of Technology, Georgia, 1998

Thesis

presented in partial fulfillment of the requirements
for the degree of

Masters of Science
in Chemistry

The University of Montana
Missoula, MT

Autumn 2006

Approved by:

Dr. David A. Strobel, Dean
Graduate School

Dr. Kent Sugden, Chair
Chemistry

Dr. Brooke Martin
Chemistry

Dr. Michele McGuirl
Division of Biological Sciences

Mintz, Kathryn, M.S., December 2006 Chemistry

ALTERATION OF DNA – TRANSCRIPTION FACTOR INTERACTIONS FOLLOWING CHROMIUM EXPOSURE

Chairperson: Dr. Kent Sugden

The effect of 8-oxoguanine in the consensus sequence of κB DNA on the binding affinity of p50BD was determined using a 22-mer and a 30-mer double-stranded DNA oligonucleotide containing the NF-κB binding site. The addition of a carboxyl moiety at position 8 on guanine (creating 8-oxoguanine) was observed to change the binding affinity of the transcription factor for the κB DNA sequences at each modified guanine site. The protocol used a p50 binding domain protein (residues 23 to 366 from the p50 protein) and a p50 mutant protein with a single amino acid mutation of the wild type histidine 67 to alanine 67. Both proteins were cloned as N-terminal his_6-tagged proteins. These proteins were expressed and purified as active proteins. It is known that reduction of chromium(VI) to chromium(III) creates species such as chromium(V) and chromium(IV) which interact with and damage DNA. An oxidative event, such a chromium(VI) reduction to chromium(III) could allow a crosslinking of protein-bound DNA. Redox values suggest that oxidative damage can travel to guanine-rich sites, such as that of the consensus sequence of κB DNA. This suggested a mechanism by which a chromium oxidative event could crosslink the DNA and protein into a binary complex without direct chromium involvement at the site of oxidation. Furthermore the protein, tightly bound to DNA, may compete with water to act as a nucleophile on DNA. This binary DNA-protein complex may be covalently linked and resistant to harsh conditions, allowing it to be visualized by HPLC or gel electrophoretic mobility shift assays. Under our conditions, no κB DNA, either unmodified or modified with 8-oxoguanine, was found to be bound to the p50BD protein. DNA oxidation through chromium reduction was not found to result in crosslinked p50BD protein in a binary DNA—protein complex.

Table of Contents

Tables

List of Figures

List of Figures - Continued

List of Abbreviations

Abbreviation	Description
NF-κB	family of proteins first discovered in the nuclear factor of the κ-light chain of B cells
p50BD	p50 protein cleaved with only the binding domain remaining
p50H67A	mutant of p50BD protein with histidine to alanine mutation
ssDNA	single stranded DNA
dsDNA	double stranded DNA
MM	molecular marker
W1, W2	wash 1 and wash 2
E1, E2	elution 1 and elution 2
8-oxoG	8-oxoguanine
22G1	22-mer κB DNA modified at guanine position 1
22G2	22-mer κB DNA modified at guanine position 2
22G3	22-mer κB DNA modified at guanine position 3
22G4	22-mer κB DNA modified at guanine position 4

CHAPTER 1

Introduction/Background

To explain what causes the initiation of cancer using a model other than the mutation model, pieces of the puzzle must be assembled one at a time. For age related diseases, such as cancer, these model pieces include chromium as an oxidant, damaged DNA, and a transcription factor protein.

Chromium background and chromium oxidation

The discovery of chromium is attributed to Vaquelin in 1798, as the mineral $PbCrO_4$ (crocoite) from Siberia,[1, 2] but its use in stainless steel could date back through history to the weapons of the Hittites (conquered by Ramsey II around 1300 B.C.).[3] The name 'chromium' stems from *chroma* (color), in reference to the wide variety of colors of chromium compounds. Although the possible oxidation states range from –2 to +6, it commonly exists in four valence states: Cr(0), Cr(II), Cr(III), and Cr(VI).[1, 4] While the anhydrous Cr(II) salts are relatively stable, the divalent state (II) oxidizes readily to the trivalent (III) state.[5]

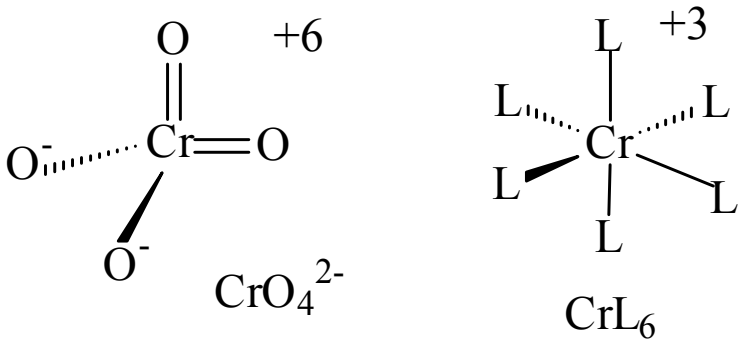

Figure 1.1: common chromium structures:
Left – Hexavalent chromium; chromate. Right – Chromium (III)

For the human body anecdotal evidence points to the +3 oxidation state of chromium to be important in the interaction between insulin and insulin receptor sites, however this has not been scientifically established. It has been established that excess chromium in the body, depending on valence states, can have unpleasant consequences including disease and death.

What is of increasing concern with regard to human health is the anthropogenic accumulation of chromium in the environment. Human chromium exposure is found

both in the workplace and in the environment. Occupational exposures to chromium can be found in welding, leather and chrome plating workers as well as stainless steel and chrome pigment production.[4]

The link between chromium and cancer was established in the late 1800s with the observation of nasal tumors in Scottish chrome pigment workers. Lung cancers were first documented in the early 1930s in German chromate workers.[1] Chromium (III) can cause toxic effects if these particles enter the respiratory tract and lungs and act as non-specific irritants.[6] The particles are unable to penetrate membranes which results in a low uptake of Cr(III) into cells. The carcinogenic form of chromium was found to be the +6 oxidation state, with lung cancer as the most prevalent outcome from inhalation exposure.[7, 8] Hexavalent chromium enters cells through phosphate and sulfate channels or by phagocytosis. The +6 oxidation state is the second most stable state after the +3 state,[5] and it is susceptible to reduction in cellular systems.[9] While Cr(VI) does not interact with DNA directly, there are a number of cellular reductants including glutathione, ascorbate, cysteine, glutathione reductase, and carbohydrates that reduce Cr(VI) to Cr(III).[6, 10] With either a concentration gradient of higher anions outside the cell's membrane or the cells need for anions such as sulfate and phosphate, the Cr(VI) enters through the anion channels, and is reduced to Cr(III); a concentration gradient is maintained and the cycle repeats. In this method the cell can accumulate extremely high levels of chromium.[11]

Hexavalent chromium, Cr(VI), is currently listed as "carcinogenic to humans" by the International Agency for Research on Cancer (IARC) and the US Toxicology Program.[12] Chromium metal and Cr(III) compounds are rated IARC 3 whereas Cr(VI) is

IARC 1.[13] The ranking of IARC 3 is used for mixtures, agents and exposures for which the evidence is inadequate to classify carcinogenicity to humans but sufficient to conclude carcinogenicity in experimental animals. IARC 1 indicates a known human carcinogen.[14]

The reduction of Cr(VI) to Cr(III) forms intermediate redox states of Cr(V) and Cr(IV). These high-valent intermediate oxidation states of chromium are unstable and are capable of causing DNA damage.[15] Using Cr(VI) and ascorbate creates reactive chromium intermediates and radicals that cause DNA damage.[16] Intracellular accumulation of Cr(III) has been proposed to interact with DNA to yield Cr-DNA, DNA-DNA, and DNA-protein crosslinks.[15]

While the functions of normal metabolism have been postulated to be one cause of age related diseases,[17] chromium exposure and the metabolic by-products generated causing cellular damage by radicals have been postulated to be another cause of age-related diseases. Cellular metabolism of chromium has the possibility to create hydrogen peroxide (H_2O_2), hydroxyl radical (•OH), and superoxide ($•O_2^-$). These oxidants are all capable of damaging proteins, DNA, RNA and other cell components.[18] This pathway of free radical oxidants from metal exposure could likely be a cause of pathogenesis. [10, 19]

DNA structure, oxidation, and 7,8-dihydro-8-oxoguanine

To investigate the second piece of the puzzle, damage to DNA, its structure and function must be understood. The structure of DNA, deoxyribonucleic acid, was defined by Watson and Crick in 1953 as a double helix composed of ordered sequences of the nucleotide residues (the nucleotide bases are adenine (A), guanine (G), cytosine (C) and thymine (T)) linked via glycosidic bond to a five carbon sugar (2'-deoxyribose); residues are linked through phosphate moieties.[20]

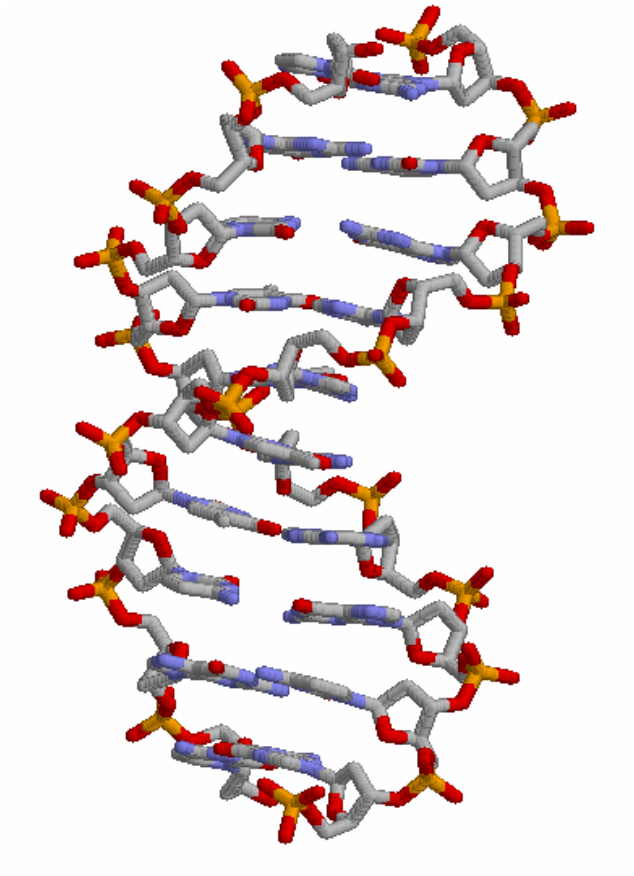

Figure 1.2: Double-stranded B-form (regular) DNA[21]

The function of DNA is to be the cell's repository of genetic information. The DNA is wrapped and packaged into chromosomes and protected in the cells nucleus. There is a basal level of DNA transcription for routine cellular needs. Additionally, in a

normal functioning cell, stimulants such as radiation and viral infections elicit a cellular response when transcription proteins bind DNA to generate RNA which can be translated into protein. The response is to fight infection or repair cellular damage.

However, in a cell with damaged DNA, these functions and mechanisms are affected. This damage to DNA includes but is not limited to DNA strand breaks and modifications to DNA. Modifications to DNA were found to primarily affect the base guanine. The one electron redox potential of guanine is the lowest of all the nucleobases at $E^{\circ} \approx 1.29$ (V vs. NHE) at pH 7. The other bases have higher redox potentials; A ≈ 1.42, C ≈ 1.6, T ≈ 1.7 (for the nucleoside forms, etc.).[18] The more negative a number, the less likely it is to be reduced and more likely it is to be oxidized. The reactivity of guanines toward any oxidant is also sequence specific. When guanine is located next to a purine — especially another guanine — it is more reactive than if it was next to a 3' pyrimidine. Furthermore, if the sequence is increased to contain more than just two guanines (G), then the reactivity also increases. Interestingly, chromium interacts preferentially at regions of high guanine content in double stranded DNA with GC ≈ GT < GA < GG < GGG < GGGG (where G is the site of damage).[22] This phenomenon is explained by a mechanism in which the highest occupied molecular orbital (HOMO) resides on the 5'G due to π-stacking in the purine runs.[23] Furthermore, this site may act as an electron hole since oxidative damage along DNA can migrate to this location. Electron hole migration is known to occur in double-stranded (ds)DNA strands, where the electron hole can "travel" through DNA up to 300 base pairs to a site of high guanine content.[24]

Oxidative damage to DNA is common. Over 100 oxidatively modified bases have been identified in DNA,[25] and these are estimated to occur at a frequency of 10,000 per cell daily for a human cell.[15, 17] This oxidative DNA damage has been separated into four distinct classes, 1) abasic sites, 2) strand breaks, 3) modified bases, and 4) DNA—protein crosslinks.[26] It has been suggested ~ 1 per 40,000 guanines in the human genome are oxidized to 7,8-dihydro-8-oxo-guanine (8-oxoguanine).[26] It appears safe to assume that 8-oxoguanine is present constitutively in every cell.

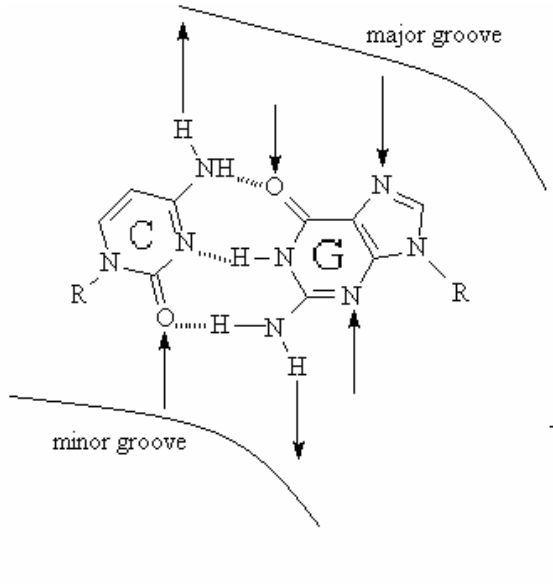

Figure 1.3A: Normal C-G base pair

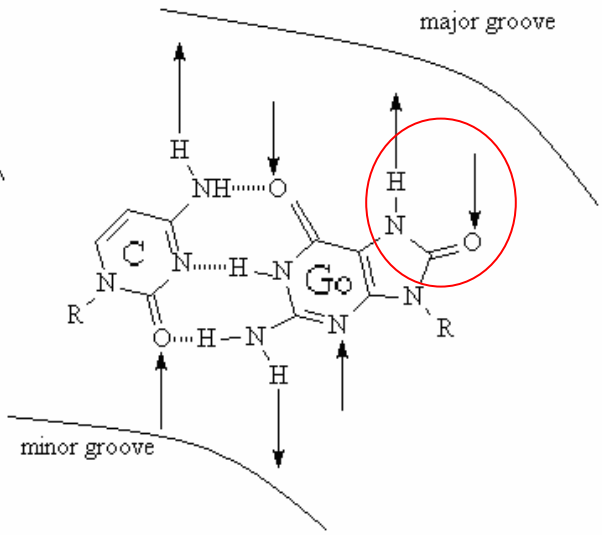

Figure 1.3B: C-8-oxoguanine base pair, with new donor/acceptor patterns

8-oxoguanine is a common guanine product under oxidizing conditions, which includes chromium exposure.[18] The normal base pairing of guanine appears, with donor acceptor patterns (figure 1.3A, from L→R), as hydrogen bond donor, acceptor, and acceptor in the major groove (in Lewis acid/base form). However, 8-oxoguanine changes the major groove donor/acceptor pattern and adds an additional acceptor bond (figure 1.3B). The specific effect of the oxidation on guanine at C8 is that the N7 transforms

from H-bond acceptor to donor, and the C8 becomes a strong H-bond acceptor at the oxygen (circled in red). The minor groove, as marked above, does not change in donor/acceptor patterns.

8-oxoguanine in the sequence 5'-CCA G^{o}CG CTGG-3', where G^{o} represents 8-oxo modification, was crystallized in 1995 by Lipscomb, et al. (183D.pdb).[27] The divergence in structure between a regular guanine versus 8-oxoguanine is very slight in an oligomer. The only change discerned when 8-oxoG containing DNA was overlaid with the same sequence DNA was in residue 4 (G^{o}) seen in the torsion angle χ from O4'-C1'-N9-C4 (the glycosidic bond region) for the guanine residue location of interest.

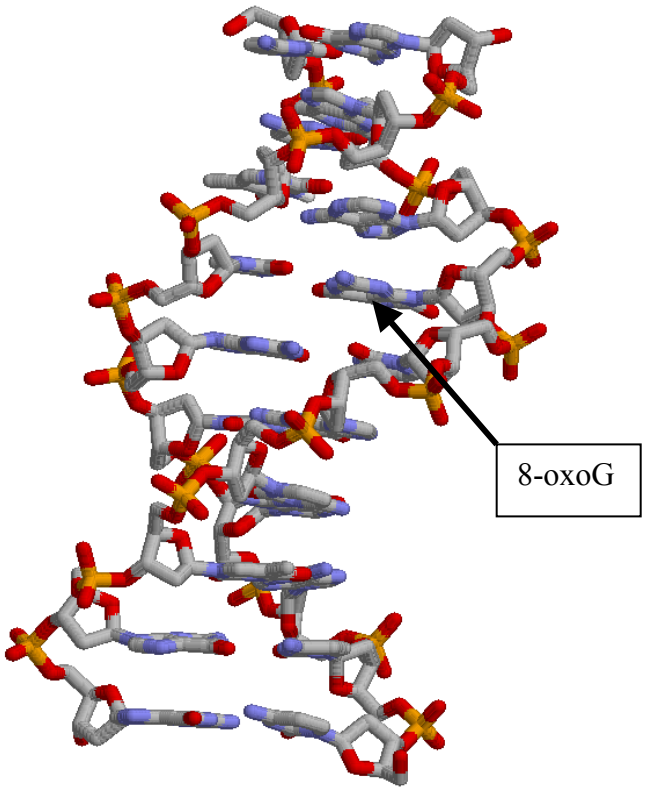

Figure 1.4: 8-oxoguanine-containing double-stranded B-form DNA[21] 183D.pdb,[27] the 8-oxo moiety tucked behind the sugar is accessible in the major groove.

Further oxidized lesions

The oxidative product of guanine, 8-oxoguanine, is prone to further oxidation.[28] Studies on the one electron redox potential for 8-oxoguanine nucleoside suggest $E^\circ \approx 0.58$ V vs. NHE at pH 8, less than that of guanine at pH 7, where $E^\circ \approx 1.29$.[18] The factors influencing the location-dependent guanine oxidation (5'-GGGG-3') will also influence 8-oxoguanine further oxidation.

With water as the nucleophile attacking at the C5 position on 8-oxoguanine, recent studies have indicated that guanidinohydantoin (Gh) and spiroiminodihydantoin (Sp) are the major products of 8-oxoguanine oxidation (by chromium(VI)).[29] The chemical structures of these further oxidized lesions are shown below, with the C5 locations indicated by arrows:

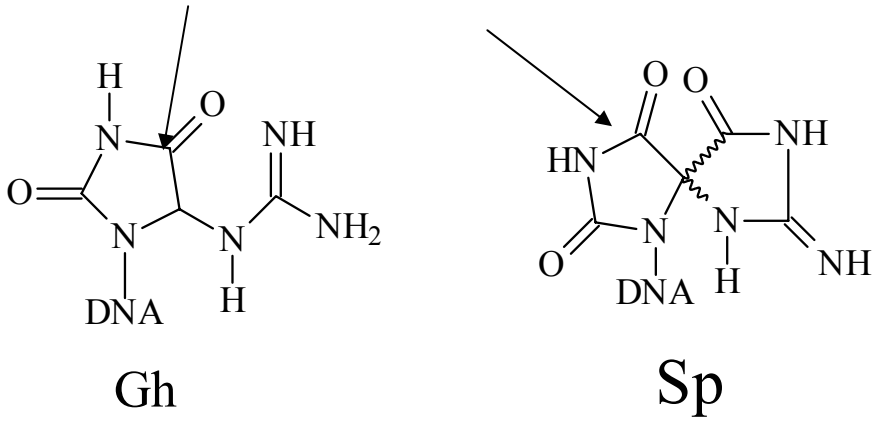

Figure 1.5: Nucleophilic attack by water at C5 of 8-oxoguanine produce Gh and Sp

Transcription factor protein chemistry

To understand DNA—protein binding and the altered protein binding affinities with damaged DNA, transcription factor protein (TFP) biochemistry must be understood. DNA—transcription factor protein interactions drive the sequence-specific nature of TFP binding. TFPs can be split into two distinct categories, the general and the sequence specific.[30] General TFPs employ cellular machinery, including RNA polymerase, that bind based on the promoter 'start' sequence of the TATA box AT-rich region. Unlike the general TFPs, specific TFPs bind to particular motifs in the sequence of the promoter region of the gene and then utilize the general TFP machinery.

Upon binding, the protein's amino acids make specific hydrogen and electrostatic bonding interactions. Examples are histidine with a positively charged (acidic) residue containing an imidazole ring, and lysine, protonated under physiological conditions. Both amino acid residues are involved in hydrogen bond interactions.

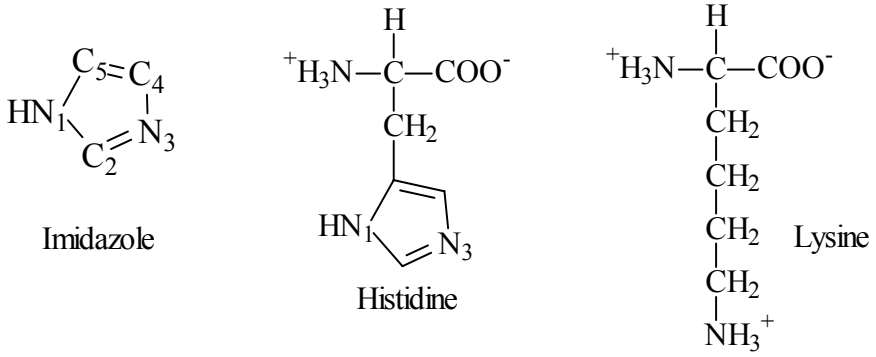

Figure 1.6: Charged structures with potential to crosslink DNA

Many TFPs have been well characterized, specifically AP-1, p53, and NF-κB which are classified as (oncogenic) activating protein, tumor suppressor protein, and signal transducer protein respectively.[30, 31, 32] The balance of activation or inactivation of

regulation is complex; either action in excess ostensibly leads to tumorigenesis. Mutations in transcription factor proteins, depending on the location, have the potential to produce severe cellular consequences, eventually resulting in disease or death. However, the exact genetic causes of disease cannot always be neatly explained by a conventional mutation model. What is known for certain is that when control is lost over gene expression, specifically the DNA—protein binding, the impact is seen in the gene product.

It has emerged that several tightly controlled regulatory DNA elements of a cell, such as the genes for NF-κB and p53, contain a consecutive run of guanines in their promoter sites and that these areas are redox sensitive.[33, 34] Many of these promoters drive genes that are transcribed during an oxidative attack on DNA. Conserved guanine sequences within promoter sites can be considered an evolutionary design to modulate gene expression during an oxidative event rather than an evolutionary 'flaw'. Logic dictates that there is a reason that DNA has evolved to have these oxidation-prone run of guanine regulatory elements. It is possible that the oxidized sequences recruit proteins based on of the type of the modification, in a similar mode to non-modified sequences which recruit transcription factor proteins based on cellular needs.

Covalent crosslinking

DNA-protein binding has been investigated for many decades. Mammalian DNA-protein crosslink existence was established in the late 1980s.[35] Much is known about chromium reactions within a cell;[6] it is established that Cr(VI) is carcinogenic and that a reduced form of chromium(VI) creates DNA-protein crosslinks, but the mechanism of how crosslinks are formed remains a mystery. Determining the exact role of chromium, Mattagajasingh and Misra suggested that, "…the nature of chromate-induced DNA-protein crosslinks is not fully resolved."[36] Currently chromium is thought to form ternary adducts with DNA in cellular systems.[6, 36, 37, 38] In this conventional model only Cr(III) is directly involved in the crosslink and both DNA and proteins are thought to be ligands of the chromium metal complex.[37]

The theory of Mattagajasingh and Misra was that intracellular reduction of Cr(VI) to Cr(III) creates species such as chromium(V) and chromium(IV), and reactive oxygen species. These species mediate the crosslinks directly in ternary structures: DNA-Cr-protein, where the DNA and the protein are metal ligands. Recent papers further propose that reduced forms of chromium are unstable crosslinks; that Cr(V) and Cr(IV) will not be found in stable ternary covalent crosslinks.[38] Yet many factors at the DNA-protein interface could allow a chromium oxidative event to crosslink the DNA and protein without direct chromium involvement. Therefore, in the reduction of the forms of Cr(V) or Cr(IV) to Cr(III), the DNA could be oxidized at the protein hydrogen-bound 8-oxoguanine DNA thereby covalently crosslinking the DNA—protein in a binary complex, rather than a ternary complex.

Many pieces of the puzzle come together to form a theory supporting a binary covalent crosslink of DNA and protein. First, it has been seen that modified DNA can recruit and hydrogen bond protein. When protein is bound to modified DNA it potentially excludes the water – the nucleophile required to generate Gh or Sp under further oxidizing conditions. Next, chromium can interact preferentially at these gene promoter regions of DNA with high guanine content, based on the redox potentials of both the chromium and the guanine-rich area, and further oxidize the DNA. Consequently, when chromium performs an oxidative event on the modified DNA, the protein can act as a nucleophile, and the oxidation could potentially crosslink the DNA—protein together in a binary complex. The theory that this binary complex is created from covalent crosslinking of modified DNA to protein by chromium oxidation incorporates two of the classes of oxidative DNA damage (the modified base and the DNA—protein crosslink). This binary covalent linkage may also block transcription by shielding the modified base from repair which would have a long-term impact on global gene expression. The binary covalent link would explain the initial causes of disease states beyond that of the simplified mutation model. Furthermore, this method of DNA—protein crosslinking explains a role of chromium in oxidative events.

Investigations into DNA—protein crosslinking

The investigations performed to elucidate the exact mechanism of crosslinks have involved an NF-κB DNA oligonucleotide, lab-generated protein, and several species of chromium. The dsDNA oligonucleotide has a run of four guanines; the non-modified (control) strand is utilized along with versions of a single modified guanine in each of the four sites.

The first step in elucidating crosslinks was to determine the electrostatic and hydrogen bond interactions of the protein with each of the dsDNA strands. Once established, the chromium species could be added to determine the effect of chromium oxidation on non-modified DNA—protein as well as modified DNA—protein binding. To determine that bonding was covalent rather than electrostatic, a denaturing environment was used to select for covalent bond resistance to degradation.

[1] Barceloux, D.G. (1999) Chromium. *Clin. Toxicol.* **37**(2), 173-194.

[2] Greenwood, N.N. and Earnshaw, A., Chemistry of the Elements. 1993, Oxford: Pergamon Press.

[3] Langård, S., ed. Biological and environmental aspects of chromium. 1982, Amsterdam: Elsevier Biomedical Press.

[4] Cohen, M.D., Kargacin, B., Klein, C.B., and Costa, M. (1993) Mechanisms of chromium carcinogenicity and toxicity. *Crit. Rev. Toxicol.* **23**(3), 255-281.

[5] Occupational Safety and Health Administration (OSHA), Department of Labor (2006). Occupational exposure to hexavalent chromium. Final rule. *Fed. Register*, 71(39), 10099-10385.

[6] Zhitkovich, A. (2005) Importance of chromium—DNA adducts in mutagenicity and toxicity of chromium(VI). *Chem. Res. Toxicol.* **18**(3), 3-11.

[7] Ewis, A.A., Kondo, K., Dang, F., Nakahori, Y., Shinohara, Y., Ishikawa, M., and Baba, Y. (2006) Surfactant protein B gene variations and susceptibility to lung cancer in chromate workers. *Am. J. Indust. Med.* **49**, 367-373.

[8] Halasova, E., Baska, T., Kukura, F., Mazurova, D., Bukovska, E., Dobrota, D., Poliacek, I., Halasa, M. (2005) Lung cancer in relation to occupational and environmental chromium exposure and smoking. *Neoplasma* **52**(4), 287-291.

[9] Shriver, D.F., Atkins, P., and Langford, C.H., Inorganic Chemistry, 2nd Ed. 1994, New York: W.H. Freeman and Co.

[10] Kasprzak, K.S. (2002) Oxidative DNA and protein damage in metal-induced toxicity and carcinogenesis. *Free Radic. Biol. Med.* **32**(10), 958-967.

[11] Sehlmeyer, U., Hechtenberg, S., Klyszcz, H., and Beyersmann, D. (1990) Accumulation of chromium in Chinese hamster V79-cells and nuclei. *Arch. Toxicol.* **64**(6), 506-508.

[12] http://monographs.iarc.fr/ENG/Classification/Listagentsalphorder.pdf

[13] http://hazmap.nlm.nih.gov/cgi-bin/hazmap_generic?tbl=TblAgents&id=7

[14] http://www.iarc.fr/

[15] Valko, M., Rhodes, C.J., Moncol, J., Izakovic, M., Mazur, M. (2006) Free radicals, metals and antioxidants in oxidative stress-induced cancer. *Chem. Biol. Interact.* **160**(1), 1-40.

[16] Stearns, D.M., Kennedy, L.J., Courtney, K.D., Giangrande, P.H., Phieffer, L.S., Wetterhahn, K.E. (1995) Reduction of chromium (VI) by ascorbate leads to chromium-DNA binding and DNA strand breaks in vitro. *Biochemistry*. **34**(3), 910-919.

[17]Ames, B., Shigenaga, M. and Hagen, T. (1993) Oxidants, antioxidants, and the degenerative diseases of aging. *Proc. Natl. Acad. Sci. USA* **90**, 7915-7922. #2

[18] Burrows, C.J. and Muller, J.G. (1998) Oxidative nucleobase modifications leading to strand scission. *Chem. Rev.* **98**(3), 1109-1152.

[19] Halliwell, B. and Gutteridge, J.M.C. Free Radicals in Biology and Medicine, 3rd Ed. 1999, Oxford: Oxford University Press.

[20] Watson, J.D. and Crick, F.H. (1953) Molecular structure of nucleic acids: a structure for deoxyribose nucleic acid. *Nature,* 4356 (April 25, 1953).

[21] Berman, H.M., Westbrook, J., Feng, Z., Gilliland, G., Bhat, T.N., Weissig, H., Shindyalov, I.N., Bourne, P.E. (2000) The Protein Data Bank. *Nucleic Acids Res.* **28**: 235-242.

[22] Borges, K.M. and Wetterhahn, K.E. (1989) Chromium cross-links glutathione and cysteine to DNA. *Carcinogenesis* **10**(11), 2165-2168.

[23] Saito, I., Takayama, M., Sugiyama, H., Nakatani, K. Tsuchida, A., Yamamoto, M. (1995) Photoinduced DNA cleavage via electron transfer: demonstration that guanosine residues located 5' to guanine are the most electron-donating sites. *J. Am. Chem. Soc.* **117**, 6406-6407.

[24] Hall, D.B., Holmlin, R.E., Barton, J.K. (1996) Oxidative DNA damage through long-range electron transfer. *Nature* **382** 731-735.

[25] Hoeijmakers, J.H.J. (2001) Genome maintenance mechanisms for preventing cancer. *Nature* **411**, 366-374.

[26] Cadet, J., Berger, M., Douki, T., and Ravanat, J.-L. (1997) Oxidative damage to DNA: formation, measurement, and biological significance. *Rev. Physiol. Biochem. Pharmacol.* **131**, 1-87.

[27] PDB ID: 183D.

Lipscomb, L.A., Peek, M.E., Morningstar, M.L., Verghis, S.M., Miller, E.M., Rich, A., Essigmann, J.M., and Williams, L.D. (1995) X-ray structure of a DNA decamer containing 7,8-dihydro-8-oxoguanine. *Proc. Natl. Acad. Sci. USA* **92**, 719-723.

[28] Prat, F., Houk, K.N., and Foote, C.S. (1998) Effect of guanine stacking on the oxidation of 8-oxoguanine in B-DNA. *J. Am. Chem. Soc.* **120**, 845-846.

[29] Niles, J.C., Wishnok, J.S. and Tannenbaum, S.R. (2004) Spiroiminodihydantoin and guanidinohydantoin are the dominant products of 8-oxoguanosine oxidation at low fluxes of peroxynitrite: mechanistic studies with ^{18}O. *Chem. Res. Toxicol.* **17**, 1510-1519.

[30] Sun, Y. and Oberley, L.W. (1996) Redox regulation of transcriptional activators. *Free Rad. Biol. & Med.* **21**, 335-348.

[31] Hess, J., Angel, P., and Schorpp-Kistner, M. (2004) AP-1 subunits: quarrel and harmony among siblings. *J. Cell Sci.* **117**(25), 5965-5973.

[32] Ho, W.C., Fitzgerald, M.X., and Marmorstein, R. (May 22, 2006) Structure of the p53 core domain dimer bound to DNA. *J. Biol. Chem.* Epublished ahead of print.

[33] Baldwin, A.S., Jr., and Sharp, P.A. (1987) Binding of a nuclear factor to a regulatory sequence in the promoter of the mouse H-2κB class I major histocompatibility gene. *Mol. Cell. Biol.* **7**(1), 305-313.

[34] Parks, D., Bolinger, R., and Mann, K. (1997) Redox state regulates binding of p53 to sequence-specific DNA, but not to non-specific or mismatched DNA. *Nucleic Acids Res.* **25**(6), 1289-1295.

[35] Oleinick, N.L., Chiu, S.-M., Ramakrishnan, N., and Xue, L.-Y. (1987) The formation, identification, and significance of DNA-protein cross-links in mammalian cells. *J. Cancer* **55**, 135-140.

[36] Mattagajasingh, S.N. and Misra, H.P. (1996) Mechanisms of the carcinogenic chromium(VI)-induced DNA-protein cross-linking and their characterization in cultured intact human cells. *J. Biol. Chem.* **271**(52), 33550-33560.

[37] Zhitkovich, A., Shrager, S., and Messer, J. (2000) Reductive metabolism of Cr(VI) by cysteine leads to the formation of binary and ternary Cr-DNA adducts in the absence of oxidative DNA damage. *Chem. Res. Toxicol*. **13**, 1114-1124.

[38] Mattagajasingh, S.N. and Misra, H.P. (1999) Analysis of EDTA-chelatable proteins from DNA-protein crosslinks induced by a carcinogenic chromium(VI) in cultured intact human cells. *Mol. Cell. Biochem.* **199**, 149-162.

CHAPTER 2

p50 Protein background and interactions:

History of NF-κB:

Nuclear factor of the κ-light chain of B cells (NF-κB) controls gene expression through recognition of κB sequences in the promoter regions of DNA.[1] The NF-κB family of proteins are transcription factor proteins that regulate a wide range of responses to infection and inflammation. The proteins mediate cell proliferation, cell transformation, angiogenesis, cell invasion, cell immunity, apoptosis, and hematopoiesis.[2] NF-κB is part of a larger family of Rel proteins, containing Rel homology domains that bind DNA as hetero- or homodimers in the nucleus.[3] The active dimer exists in an inactive state as a heterotrimer in the cytoplasm where the dimer is bound with an IκB inhibitor protein (IκB-α, IκB-β, IκB-γ, Bcl-3, and *cactus*). Activation causes phosphorylation and ubiquitination of the inhibitory protein and the free NF-κB dimer then translocates into the nucleus. The five members of the NF-κB are p65 (RelA), RelB, c-Rel, p50 (NF-κB1) and p52 (NF-κB2). The most common NF-κB protein is the p50/p65 heterodimer.[4]

The proteins bind DNA sequences, called κB DNA enhancer elements. The generic κB DNA consensus site, which will bind all NF-κB proteins, has been determined to be a ten base pair sequence, 5'-GGG RNW YYC C-3' (where N is any nucleotide, Y is pyrimidine, R is purine, and W is A or T).[5] Hundreds of variations of this κB DNA sequence exist in gene promoters.[5] Most dimers can associate with varying binding affinities to different κB DNA sites. These small differences in binding affinities for κB sequences can have an impact on the expression of genes, implying that the role of the

DNA sequence and its conformation has an important responsibility in gene expression with the NF-κB protein.[5] Huang et al. proposed to organize the κB sites into two distinct classes, class I for p50 and p52 hetero- and homodimer binders, and class II for p65 and c-Rel hetero- and homodimers.[5]

The ten base pair consensus sequence contains the class I κB site of 5'-GGG RN-3' half-site and the class II κB site of 5'-YYCC-3' half-site. The most 5'-G for class I κB is in contact with a histidine side chain that is exclusive to p50 and p52 which gives rise to sequence specificity. For p65 and c-Rel, the histidine in the protein sequence is replaced with an alanine. The impact for these sequence specificities is that the homodimers of p50 and p52 bind optimally to 11 base pair κB sites, heterodimers with p50 or p52 prefer 10 base pair sites, and homodimers of p65 or c-Rel prefer 9 base pair κB sites.[5]

Ghosh et al.[6] and Müller et al.[7] crystallized residues 39-364 for the mouse p50 protein and residues 2-366 for the human p50 protein, respectively. For Ghosh et al., these truncated protein constructs bound both the κB sequence and I-κB. For Müller et al. the truncated protein was the most stable fragment that was proteolytically cleaved from p105 to create p50 ending at the nuclear localization signal (Figure 2.1).

The Rel homology domain folds into two subunits, the larger N-terminal domain which contacts DNA base pairs and the smaller C-terminal domain which is responsible for dimer formation and DNA phosphate contact. Residue proline 43 marks the beginning of the Rel homology domain; residues 160-205 form an α-helical like structure within the Rel domain but are not part of the domain. Residues 250 – 366 mark the C-terminal domain and residue 366 marks the end of the nuclear localization signal.

Residues 244-250 form a flexible linker region between the two domains which is not stabilized by H-bonds or hydrophobic contacts which makes it ideal as a flexible hinge for the protein to bind to or dissociate from DNA.

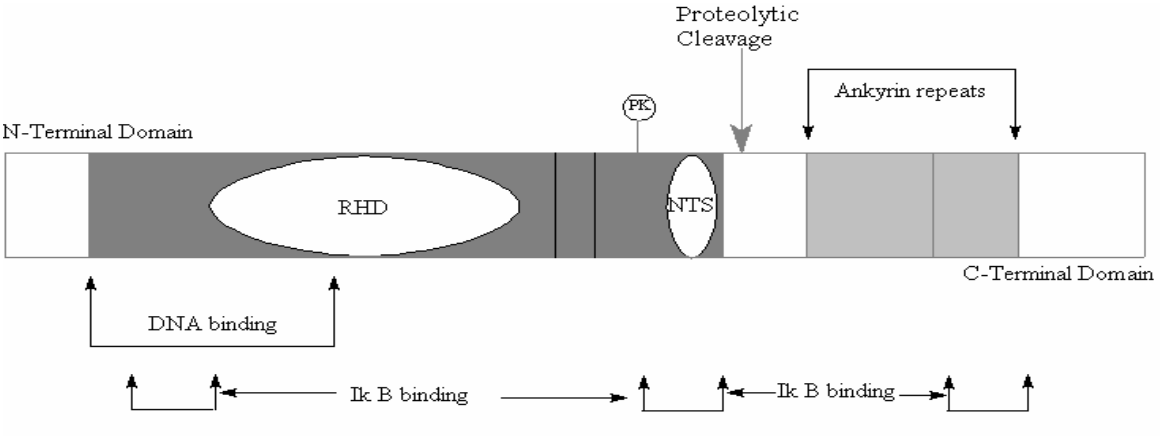

Figure 2.1: Structure of p105/p50 Adapted from Gilmore, et al. (1996) *Oncogene* **13**, 1367-1378.[8] RHD – Rel Homology Domain; PK – protein kinase A recognition sequence; NTS – nuclear targeting sequence also known as nuclear localization signal. Protease cleaves as indicated to form p50 from p105, leaving the N-terminus intact.

DNA recognition

Both the N- and the C-terminus contact DNA. The protein binds in the major groove and in the p50 homodimer, at the dimer interface, the C-terminus domains wrap around the DNA for phosphate interactions. The N-terminal domain covers the 5'-GGGGAC-3' half site. The C-terminal domain is composed of six variable loops. The N-terminal domain contains nine variable loops, two of which comprise the κB DNA recognition loops, allowing for flexibility in protein conformation and binding DNA. The N-terminal domain does not contribute to the protein dimerization interface. Specific DNA recognition by p50 is shown in Figure 2.2, page 23. When p50 binds DNA, there a slight deviation from B-form DNA with the unwinding and a slight bend of DNA. There is no extreme distortion of DNA by the protein.[6]

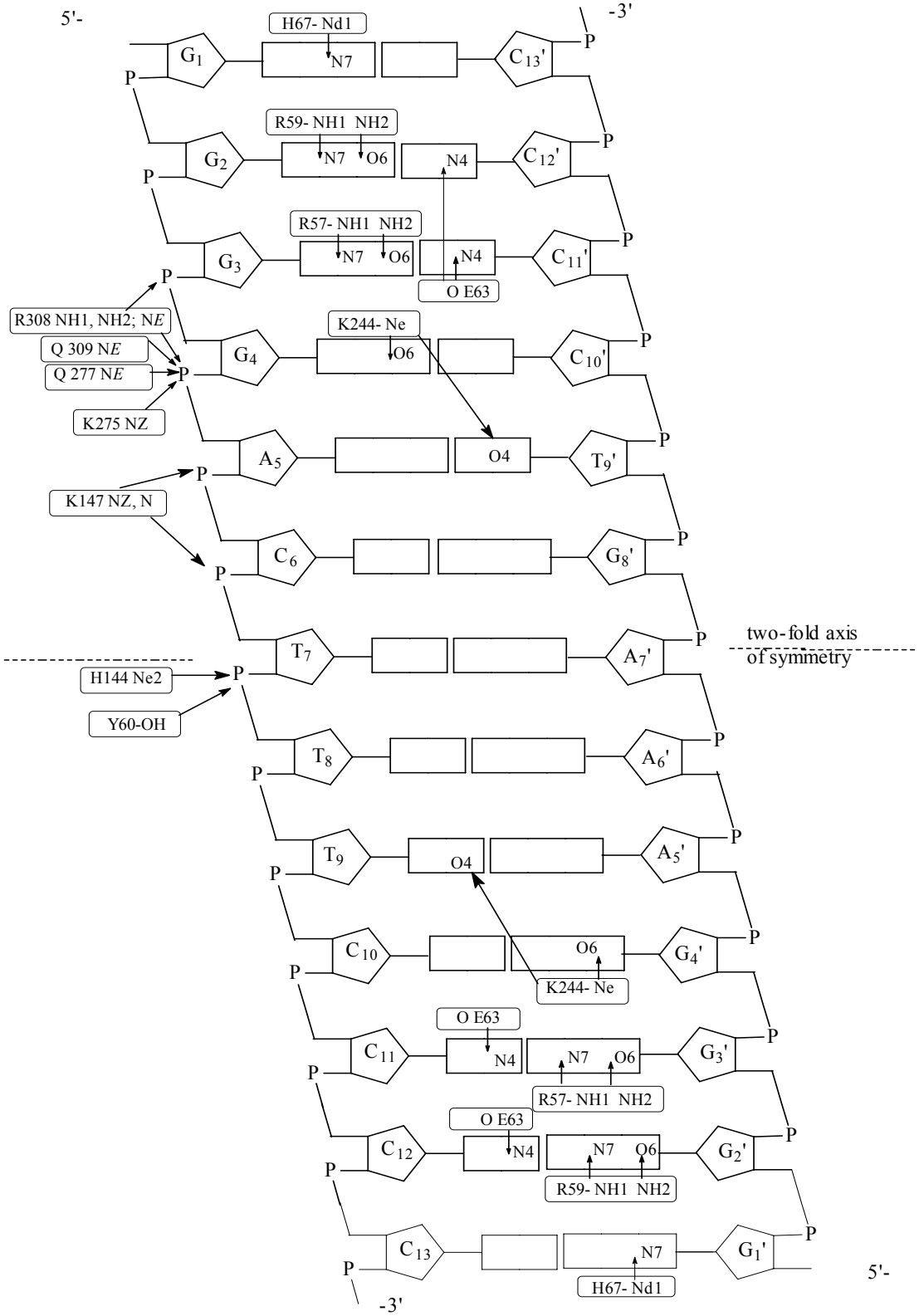

Figure 2.2: p50 protein binding κB DNA consensus sequence 5'-GGGGACTTTCCCC-3' / 5'-GGGGAAAGTCCCC-3', adapted from Ghosh, G., et al. *Nature* **373**, 303-310, and Müller, C.W., et al (1996) *Nature* **373**, 311-317. [6, 7]

Site-specific changes to p50BD to create a mutant protein

We have previously shown that a 22-mer double-stranded DNA sequence (5'-AGT TGA $G_1G_2G_3$ G_4AC TTT CCC AGC C-3') with an 8-oxoguanine in each of the numbered guanines sites gave discrete p50 protein binding affinities depending upon the location of the 8-oxoguanine lesion.[9] The histidine in position 67 of the human p50 protein is important in DNA binding as the histidine would contact the 8-oxoguanine at position G_1. The C5 of 8-oxoguanine, a vinyl carbon, could be subject to nucleophilic attack by either of the histidine's nitrogens at position 67 during an oxidative event (see Figure 2.3). As an 8-oxoguanine in specific NF-κB sequence positions could impact binding affinities, a mutant was engineered with the histidine changed to an alanine in order to mimic p65 or c-Rel binding. In addition, the engineered p50 protein consisted of only the DNA binding domain, residues 23-366.

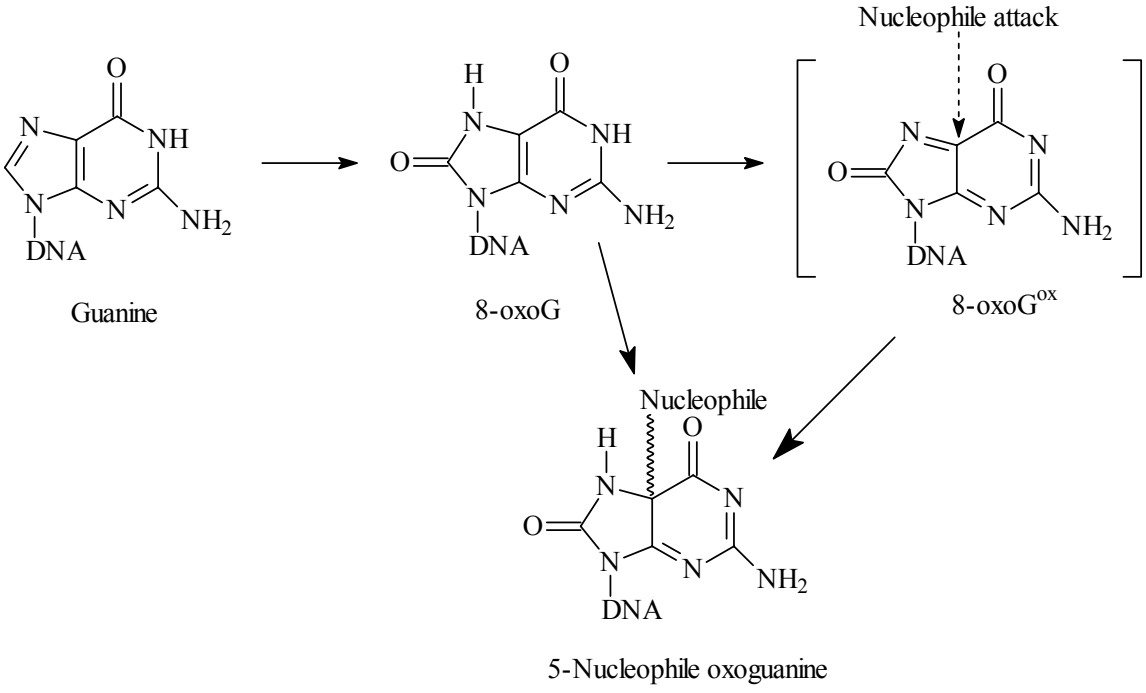

Figure 2.3: Mechanism of nucleophilic attack.

Table 2.1: DNA and protein sequence comparisons of the p50 binding domain protein and p50 mutant protein

Comparison of protein sequences	
p50BD	GAA GGC CCA TCC **CAT** GGT GGA CCT GGT
Translation of p50BD (1 letter protein code)	H T I F N P E V F Q P Q M A L P T D G P Y L Q I L E Q P K Q R G F R F R Y V C E G P S **H** G G L P G A S S E K N K K S Y P Q V K I C N Y V G P A K V I V Q L V T N G K N I H L H A H S L V G K H C E D G I C T V T A G P K D M V V G F A N L G I L H V T K K K V F E T L E A R M T E A C I R G Y N P G L L V H P D L A Y L Q A E G G G D R Q L G D R E K E L I R Q A A L Q Q T K E M D L S V V R L M F T A F L P D S T G S F T R R L E P V V S D A I Y D S K A P N A S N L K I V R M D R T A G C V T G G E E I Y L L C D K V Q K D D I Q I R F Y E E E E N G G V W E G F G D F S P T D V H R Q F A I V F K T P K Y K D I N I T K P A S V F V Q L R R K S D L E T S E P K P F L Y Y P E I K D K E E V Q R K R Q K L Stop Stop
P50H67A	GAA GGC CCA TCC **GCA** GGT GGA CCT GGT
Translation of p50H67A (1 letter protein code)	H T I F N P E V F Q P Q M A L P T D G P Y L Q I L E Q P K Q R G F R F R Y V C E G P S **A** G G L P G A S S E K N K K S Y P Q V K I C N Y V G P A K V I V Q L V T N G K N I H L H A H S L V G K H C E D G I C T V T A G P K D M V V G F A N L G I L H V T K K K V F E T L E A R M T E A C I R G Y N P G L L V H P D L A Y L Q A E G G G D R Q L G D R E K E L I R Q A A L Q Q T K E M D L S V V R L M F T A F L P D S T G S F T R R L E P V V S D A I Y D S K A P N A S N L K I V R M D R T A G C V T G G E E I Y L L C D K V Q K D D I Q I R F Y E E E E N G G V W E G F G D F S P T D V H R Q F A I V F K T P K Y K D I N I T K P A S V F V Q L R R K S D L E T S E P K P F L Y Y P E I K D K E E V Q R K R Q K L Stop Stop

The binding affinities for the p50 binding domain protein with the five oligonucleotide sequences, four of which contain 8-oxoguanine modifications, were investigated. For the p50H67A mutant with the control and the 8-oxoguanine DNA modified at position G1, the binding affinities were investigated. An apparent binding constant, K_{app}, was determined for each protein-DNA modification as the point where the fraction bound equals 50% graphically.

Materials and methods:

Deoxyribonucleotides. Unmodified oligonucleotides with the κB consensus sequence were obtained from IDT DNA (Coralville, IA). Modified 22-mer DNA sequences containing an 8-oxoguanine in the NF-κB protein p50 homodimer consensus sequence (5'-AGT TGA **$G_1G_2G_3$ G_4AC TTT CC**C AGC C-3', where the bold bases indicate the consensus sequence and the G_{1-4} indicate positions of 8-oxoguanines in the recognition sequence) were obtained from TriLink Biotechnologies (San Diego, CA). Modified 30-mer DNA sequences containing the sequence 5'- TCC GCT **$G_1G_2G_3$ G_4AC TTT CC**G CGG AGA CTC TAG -3' (again the bold bases indicate the consensus sequence and the G_{1-4} indicates positions of 8-oxoguanines in the recognition sequence) were also obtained from TriLink Biotechnologies. HPLC purification of the 22-mer oligonucleotide strands was performed using a Dionex DNAPac PA-100, 4 mm x 250 mm anion exchange column. Elution was accomplished with a linear gradient of 90% mobile phase A (10% aqueous acetonitrile) and 10% mobile phase B (1.5 M ammonium acetate (pH 6.2), 10% acetonitrile) to 100% mobile phase B over the course of 22 minutes. The 30-mer oligonucleotide was purified in a similar manner, however mobile phase A also contained 500 mM NaCl and elution was accomplished with a linear gradient of 90% A and 10% B to 100% mobile phase B over 30 minutes. Column elutions of oligonucleotides were observed by diode array at 268 nm. The single-peak elution of oligomer was evaporated to remove the volatile acetonitrile, eluted through a BioRad chromatography column 6 and stored at -20˚C until needed for testing. The NaCl from the 30-mer oligonucleotides was removed by elution through a BioRad chromatography column 30. Standard methods were employed to 5'- ^{32}P end-label specific oligomers. The control or 8-oxoguanine

containing single stranded DNA was incubated with polynucleotide kinase and 10 μCi of ^{32}P-γ-ATP for 30 minutes. Column elutions with a Micro Bio-Spin 6 chromatography column from BioRad (Hercules, CA) removed the enzyme and unincorporated nucleotides. The radiolabeled single stranded DNA was annealed to complement DNA by heating to 95˚C and slowly cooling 1˚C / 1 minute using a Peltier Thermal Cycler from MJ Research (BioRad, Waltham, MA).

NF-κB p50BD Transcription Factor Protein. The p50 binding domain sequence from residues 23 to 366 was created using an I.M.A.G.E. clone of the p105 protein as a PCR template. The p50 binding domain region was amplified by PCR using primers from IDT DNA. The p50BD DNA contained engineered restriction sites *Eco*R I and *Xba* I at the 5'- and -3' ends respectively. These primers were p50EcoR1H23For (5'-GGA ATT CCA TAC AAT AAT TAA TCC AGA A-3') and p50Rev (5'-AGG CTC TAG ATT TCA TCA GAG CTT CTG ACG TTT CCT-3'). The pPROEX HTa plasmid (Invitrogen) was transformed into competent GW1678, a dam$^-$ and dcm$^-$ *E. coli* strain (*E. coli* Genetic Stock Center). The *E. coli* were made competent by picking colonies from freshly streaked plates and growing overnight at 37˚C in LB media; 2 mL of the overnight culture was then grown in 100 mL of LB-media at 37˚C until OD_{260} was 0.3 to 0.4. The culture was collected in 50 mL tubes and centrifuged at 4000 rpm for 15 minutes at 4˚C, and then the liquid was drained. The pellet was re-suspended in approximately 16.5 mL solution A (100 mM RbCl, 50 mM $MnCl_2 \cdot H_2O$, 30 mM KCH_3COOH, 10 mM $CaCl_2 \cdot 2H_2O$, 15% (v/v) glycerol, pH 5.8 by 0.2 M CH_3COOH, and filter sterilized), incubated on ice for 30 minutes and centrifuged at 4000 rpm for 15 minutes at 4˚C. The pellet was re-suspended in approximately 4 mL solution B (10 mM MOPS, 10 mM RbCl, 75 mM $CaCl_2 \cdot 2H_2O$,

15% (v/v) glycerol, pH 6.8 with NaOH and filter sterilized) and incubated on ice for 15 minutes. Aliquots were distributed into microcentrifuge tubes, flash frozen in dry ice/ethanol mixture and stored at -80˚C.[10] The plasmids were amplified in this strain to provide a non-methylated plasmid as subsequent restriction enzymes are inactive on methylated DNA. The PCR insert and plasmid were cut with *Eco*R I and *Xba* I, ligated with Quick Ligase (New England Biolabs, Ipswich, MA) at room temperature for five minutes, chilled on ice, and then transformed into XL-10 Gold Ultracompetent cells (Stratagene, La Jolla, CA). The transformations were performed by mixing gently 100 µL of competent cells in ice-cold 14 ml BD Falcon polypropylene round-bottom tubes with 1.7 µL β-mercaptoethanol (1.42 M) over 10 minutes. The ligation mixture was added to the tubes (130 ng, ~3 µL) and the mixture was incubated on ice for 30 minutes. The cells were heat-pulsed for 45 seconds at 42˚C, and chilled on ice for 2 minutes. NZY^+ media (900 µL, 42˚C, NZY^+: 10 g NZ amine, 5 g yeast extract, 5 g NaCl, deionized H_2O to 1 L, pH 7.5, autoclave. Prior to use a 12.5 mL filter sterilized solution of 1M $MgCl_2$, 12.5 mL 1M $MgSO_4$, and 20 mL 20% (w/v) glucose was added and the cells were incubated at 37˚C for 1 hour with 225 rpm shaking. Approximately 200 µL competent transformed cells were spread on fresh LB-ampicillin 3% agar LB plates and incubated overnight at 37˚C. Insert verification by PCR was performed before sequencing using the procedure that follows. Ten clones that grew on the 'plasmid + insert' plate were isolated using a QIAprep kit (Qiagen, Valencia, CA). The plasmid DNA, containing insert was grown overnight in 15 mL tubes at 37˚C in LB media after picking colonies from the 'plasmid + insert' plates. The culture was centrifuged at 4000 rpm for 15 minutes at 4˚C, the liquid was drained, and the pellet was frozen at -20ºC. The plasmid DNA was isolated using a

Qiagen miniprep kit according to manufacturer's directions. The plasmid DNA concentrations for the ten clone samples were determined by measuring $OD_{260/280}$; 10 ng aliquots from each of the ten plasmid samples were PCR incubated with the forward and reverse cloning primers described earlier and then run on a 1.2% agarose gel. Two successful clones showing the insert were selected for sequencing to verify the presence of insert and to ensure the clone was error free and then transformed into BL21 (DE3) expression cells (Stratagene). Sequencing primers used were the p50EcoR1H23For, p50Rev, p50seqfor (5'-GAC AAA GTT CAG AAA-3') and p50seqrev (5'-GAT CCC ATC CTC ACA-3'). The cell transformation into the BL21 (DE3) *E. coli* was similar to the procedure for the XL-10 Gold Ultracompetent cells except the media used was room temperature SOC (20g tryptone, 5 g yeast extract, 0.5 g NaCl, deionized H_2O to 1 L, autoclave; added prior to use, filter sterilized 10 mL of 1M $MgCl_2$, 10 mL 1M $MgSO_4$, 2 mL 20% (w/v) glucose).

Protein mutations. A Quikchange® site-directed mutagenesis kit (Stratagene) was used to create the histidine to alanine mutation. This kit allows for site-directed mutagenesis in double-stranded miniprep plasmid DNA. The p50BD (binding domain) plasmid DNA was incubated with complementary oligonucleotide primers containing the mutation sequence. The forward primer H64Afor (5'-TAT GTG AAG GCC CAT CCG CAG GTG GAC TAC CTG GTG-3') and reverse primer H64Arev (5'-CAC CAG GTA GTC CAC CTG CGG ATG GGC CTT CAC ATA -3') were extended with *PfuTurbo* DNA polymerase during temperature cycling. The primers created new, mutated plasmids having nicks/non-overlapping single strand breaks that were capable of transformation into competent cells. The products were *Dpn* I endonuclease treated to remove

methylated and hemimethylated DNA (only the parental plasmid DNA is methylated). This enzyme targets 5'-G^{m}ATC-3' sequences. The final step was the vector DNA transformation into XL1-Blue supercompetent cells. Fresh LB-ampicillin 3% agar plates with IPTG (isopropylthio-β-D-galactoside) and X-gal (5-bromo-4-chloro-3-inodlyl-β-D-galactopyranoside) were prepared; the plates were incubated at 37˚C for greater than 16 hours to allow for blue colonies to evolve indicating a successful transformation. Plasmid DNA for p50H67A was isolated as described earlier and PCR incubated with the p50EcoR1H23For and p50Rev primers and run on a 1.2% agarose gel. One successful clone showing the insert was selected for sequencing to verify insert and transformed into BL21 (DE3) protein expression cells (Stratagene).

Protein purification. The expression plasmids, in BL21 (DE3) cells, were grown to an OD_{600} of 0.3-0.6 at 37˚C in LB media containing 25 μg/mL ampicillin, as the pPROEX HTa contains an ampicillin resistance cassette. Cells were induced with IPTG to a final concentration of 0.1 mM and incubated for 4 hours at 37˚C. Cells were then harvested by centrifugation at 4˚C and 5,000 rcf, and frozen at -20˚C for later use. After thawing on ice, cells were lysed using the BugBuster® protocol and reagent (Novagen, 5 mL reagent per gram wet cell paste), lysozyme (Sigma, 0.5 mg per gram wet cell paste), Benzonase nuclease (Novagen, 1 μL per mL BugBuster® reagent), and protease inhibitor cocktail (Roche, 1 tablet dissolved in 2 mL H_2O, use 0.2 mL per 5 mL extraction reagent). Cell lysate was filtered through a Ni-NTA column (Qiagen). Protein was washed with Solution A and B (50 mM NaH_2PO_4, 300 mM NaCl, with 10 mM and 20 mM imidazole respectively) and eluted with Solution C (50 mM NaH_2PO_4, 300 mM NaCl, 250 mM imidazole). The elution fraction was de-salted using a Microcon YM-10 and eluted into

protein storage buffer (20 mM HEPES, 50 mM NaCl, pH 7). An aliquot was reserved for BCA protein concentration analysis (BCA kit, Pierce, Rockford, IL), and the remaining sample was diluted in half with protein storage buffer containing 40% glycerol, aliquoted into 15-25 μL sub-samples depending on protein concentration, and stored at -80˚C.

Electromobility Shift Assay (EMSA or gelshift). DNA-protein binding reactions were performed using 2.6 μM 5'-^{32}P radioactive-labeled DNA which had been annealed to its complement to create double stranded DNA (dsDNA). The reaction buffer for the DNA-protein binding was acquired from Promega [buffer: 20% glycerol, 5 mM $MgCl_2$, 2.5 mM EDTA, 2.5 mM DTT, 250 mM NaCl, 50 mM Tris-HCL, pH 7.5, 0.25 mg/mL poly(dI-dC)]. The DNA and protein were allowed to react for 20 minutes before running on a polyacrylamide gel; either a native 4% polyacrylamide gel or a 6% Invitrogen pre-poured retardation gel. Additionally, glycerol (1 μL, 40%) was added to all reaction mixes to increase density and help with sample loading. Unless a free well was available for dye only, the sample 'DNA only' was the only well to have loading dye added in order to minimize any interference of the dye with the DNA and protein binding interactions. The gels were run at 250-300 V for ~10 minutes. The gel shifts were analyzed by autoradiography (Kodak).

Data Analysis. The EMSA analysis of binding affinity for the control and the 8-oxoguanine modified oligonucleotides was performed using GS 800 Calibrated Densitometer from BioRad, by integrating the area for each band and dividing the area of the protein-bound DNA by the total area of the free and bound DNA bands to yield a percent bound. The software used was PDQuest 2-D gel analysis software to scan the gel image and Quantity 1 analysis software to determine the physical area to integrate. The

apparent dissociation constant K_{app} was determined as the point where the fraction bound equals 50% graphically.

Results:

Cloning and mutagenesis of the p50 DNA binding domain

The p50BD PCR product ligated into pPROEX HTa was transformed into XL-10 Gold Ultracompetent cells as these cells are engineered for superior uptake efficiency of plasmid DNA. For protein expression the plasmid was transformed into BL21 (DE3) cells. The presence of the insert was confirmed by PCR using the original cloning primers to amplify an ~1000 base pair fragment from the isolated plasmid (see arrow pointing to 1000 base pair molecular marker, Figure 2.4). Six of the first ten clones (5-10, Figure 2.5) contained insert and four did not (1, 3, 4, and 11). The lane marked '0' is a template-free PCR control lane.

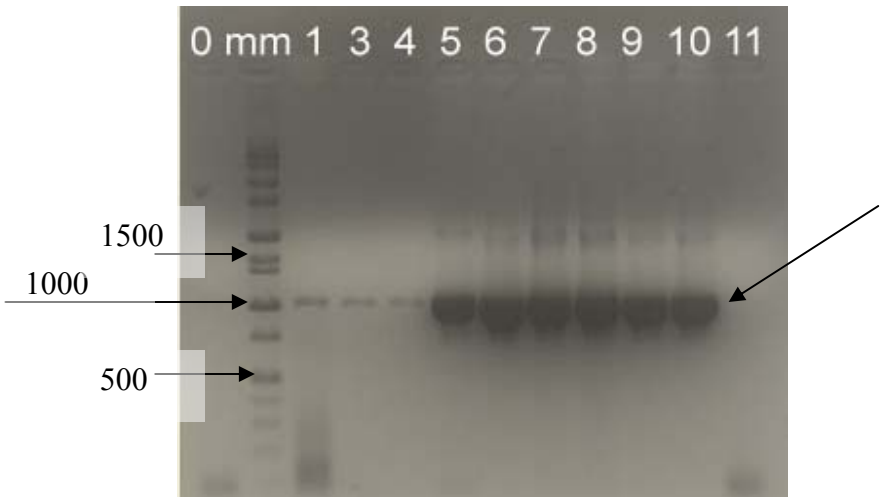

Figure 2.4: PCR of p50BD clone, arrow at molecular marker 1000 base pairs.

For the mutant of p50BD, p50H67A, to confirm the presence of insert, PCR was performed using the original p50BD cloning primers. Figure 2.5 indicates that all the clones loaded onto the gels contained insert of the correct size ~ 1000 base pairs (see arrow at 1000 base pair molecular marker). All seven clones selected (1-7, Figure 2.5) contained insert. The lane marked '0' is a template-free PCR control lane.

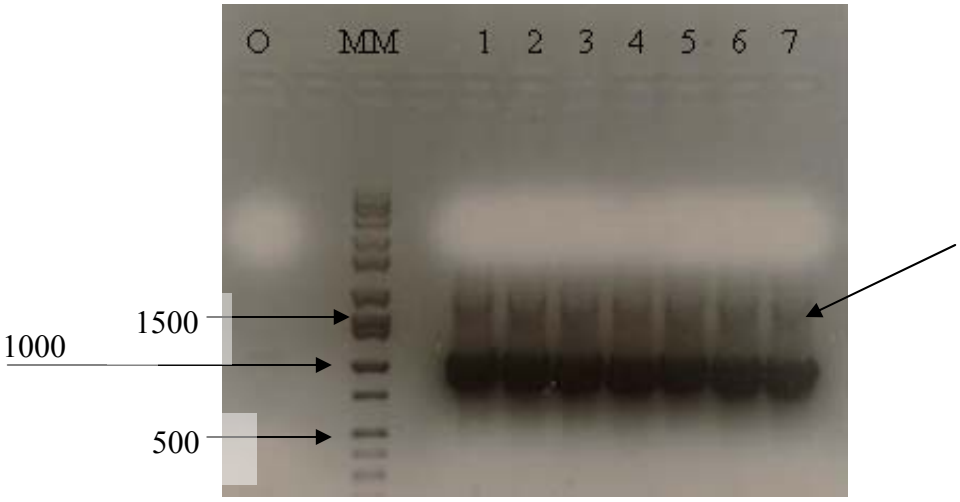

Figure 2.5: PCR of p50H67A, arrow at molecular marker 1000 base pairs.

The Chromas sequencing determined that the clone p50BD DNA was error free. The mutation DNA, p50H67A, was also found to be in agreement with the expected sequence and error free (see Table 2.1, page 25, and Figure 2.6).

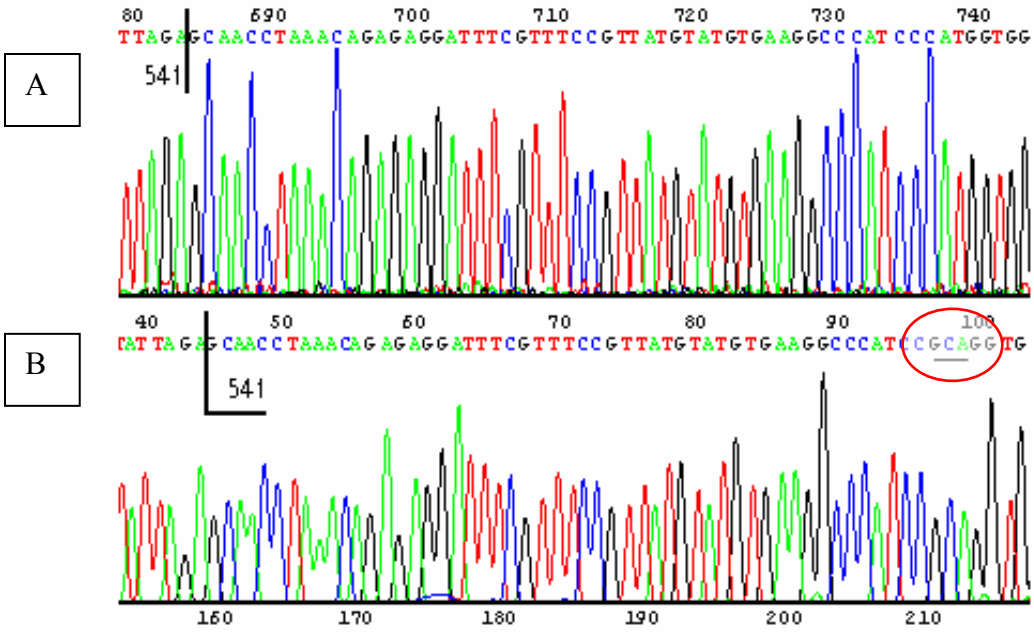

Figure 2.6: Sequence of proteins at mutation site
A: (top) sequencing of p50BD
B: (bottom) sequencing of p50H67A (area circled in red, 3 base mutations underlined).

Expression of the wild type and mutant p50BD protein

Transformed BL21(DE3) cells containing p50BD or p50H67A plasmids were grown to OD_{600} of 0.3-0.6, induced with IPTG, and incubated for 4 hours at 37˚C. The proteins were purified with a Ni-NTA column as described in Materials and Methods. The proteins were washed with Solution A and an aliquot was collected (W1 in Figure 2.7 for p50BD). The second wash, W2, of the column-bound protein with Solution B removed trace protein impurities (see W2, Figure 2.7). The protein elution was performed using two volumes of Solution C and aliquots show a band at the correct molecular weight for p50BD, 42,400 Da (band at E1 and E2, Figure 2.7). The elution fraction E1 was de-salted using a Microcon YM-10, eluted into protein storage buffer, and stored at -80˚C.

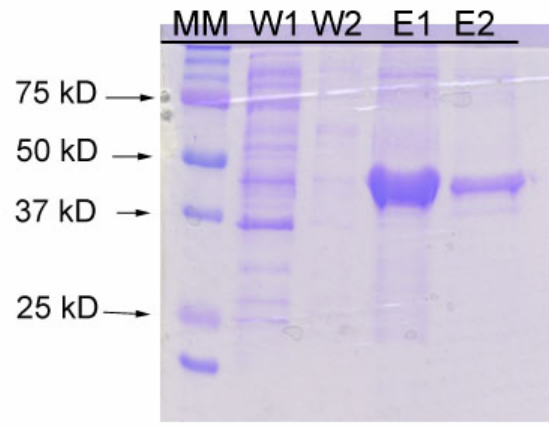

Figure 2.7: p50BD protein purification. Protein elution by imidazole at E1 and E2.

The elution of p50H67A was performed using two volumes of Solution C and aliquots show the molecular weight of p50H67A, 42,400 Da (band at E1 and E2, Figure 2.8). The elution fraction was de-salted using a Microcon YM-10, eluted into protein storage buffer, and stored at -80˚C.

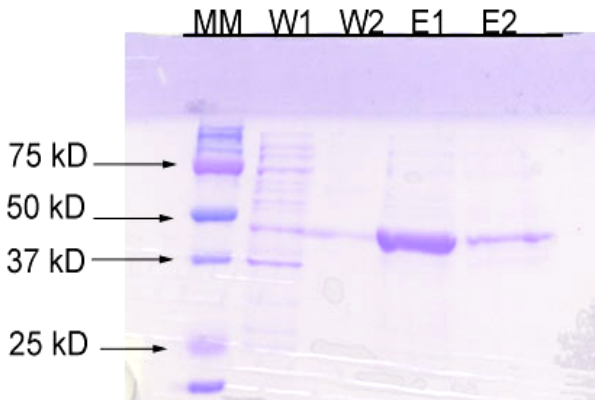

Figure 2.8: p50H67A protein purification. Purified p50H67A protein elution at E1, with some elution at W2 and E2.

DNA-protein interactions.

To investigate DNA-protein binding, oligonucleotides were ordered from IDT DNA and TriLink DNA. The "control" sequences for the 22-mer and 30-mer oligonucleotide strands represents unmodified DNA and provides a basis for determining the ratio of DNA to protein for a gel shift. The 30-mer oligonucleotide sequences were used for binding comparisons of mutant protein to wild type binding domain protein. An 8-oxoguanine modification was made at every guanine indicated by ^{O}. In this manner, each guanine in the consensus sequence had its modification evaluated by binding affinity.

Table 2.2: Sequence of 22-mer and 30-mer DNA; bold at the consensus site. Table adapted from Hailer-Morrison, et al (2003) *Biochem.* **42**, 9761-9770. [9]

Oligomer strands, ^{O} indicates 8-oxoguanine position	
22-mer control	5'-AGT TGA **$G_1G_2G_3$ G_4AC TTT CC**C AGC C-3'
22-mer modified	5'-AGT TGA **$G_1^{O}G_2G_3$ G_4AC TTT CC**C AGC C-3' 5'-AGT TGA **$G_1G_2^{O}G_3$ G_4AC TTT CC**C AGC C-3' 5'-AGT TGA **$G_1G_2G_3^{O}$ G_4AC TTT CC**C AGC C-3' 5'-AGT TGA **$G_1G_2G_3$ G_4^{O}AC TTT CC**C AGC C-3'
30-mer control	5'-AGT TGA **$G_1G_2G_3$ G_4AC TTT CC**C AGA CTC TAG-3'
30-mer modified	5'-TCC GCT **$G_1^{O}G_2G_3$ G_4AC TTT CC**G AGA CTC TAG-3' 5'-TCC GCT **$G_1G_2^{O}G_3$ G_4AC TTT CC**G AGA CTC TAG-3' 5'-TCC GCT **$G_1G_2G_3^{O}$ G_4AC TTT CC**G AGA CTC TAG-3' 5'-TCC GCT **$G_1G_2G_3$ G_4^{O}AC TTT CC**G AGA CTC TAG-3'

Interaction of the 22-mer κB-DNA oligomer control sequence with p50BD:

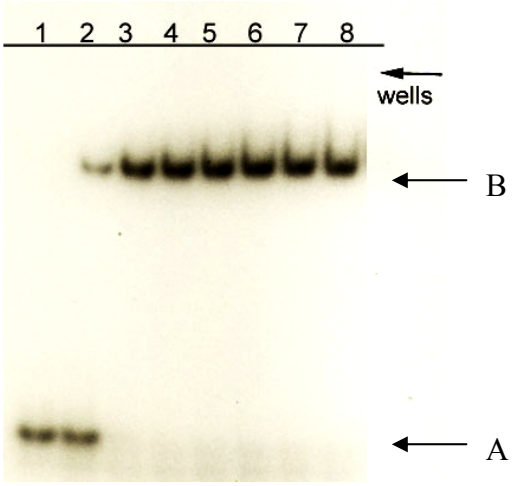

Figure 2.9: 22-control κB DNA with p50BD.
Lanes 1-8: dsDNA + p50BD (0, 0.457, 0.914, 1.37, 1.83, 2.29, 2.74, and 3.20 μM protein)

Electrophoretic mobility shift assays show DNA binding to protein visualized by autoradiography. The bound DNA-protein (arrow B in figure 2.9) is of higher molecular weight due to electrostatic/hydrogen bond interactions and this entity moves more slowly through a gel than free oligomer (arrow A in figure 2.9). Figure 2.9 also shows that the protein is active and binds to the κB DNA sequence. An approximately 50% shift of the DNA is accomplished using 0.457 μM p50BD protein (lane 2 as compared to zero shift from lane 1, no protein) and a complete shift with 0.914 μM protein (lane 3). Excess protein confirms the 100% shift of 0.914 μM p50BD (lanes 4 – 8, Figure 2.9).

Interaction of the 22-mer κB modified at G1 DNA sequence with p50BD:

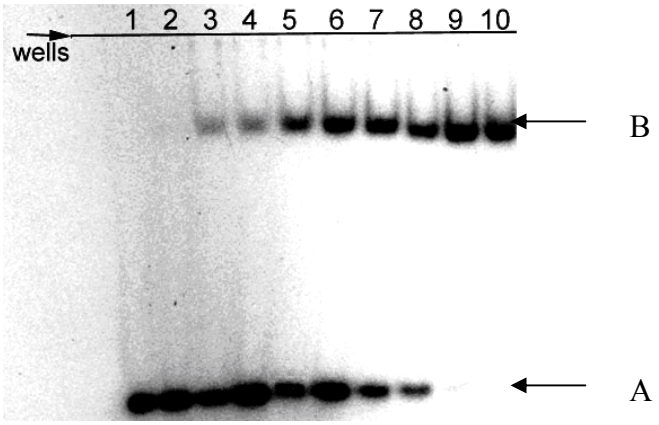

Figure 2.10: 22G1 κB DNA with p50BD.
Lanes 1-10: dsDNA + p50BD (0, 0.471, 0.942, 1.414, 1.885, 2.356, 2.827, 3.298, 3.769, and 4.241 μM protein).

The 8-oxoguanine modification at G1 for the 22 base pair oligomer (Figure 2.10) shows that the protein does not bind as well to the modified strand as it does for the control. In fact, the same amount of protein that would 100% shift unmodified κB DNA sequence – lane 3, ~ 1 μM, figure 2.9 – will only shift the 22-mer with an 8-oxoguanine at position G1 by approximately 25%. A complete shift is not seen until lane 9, with 3.769 μM of protein, which is four times as much protein as unmodified DNA requires.

Interaction of the 22-mer κB modified at G2 DNA sequence with p50BD:

Two distinct bands were observed (Figure 2.11) when p50BD protein is incubated with a 22-mer κB sequence modified in the G2 position with an 8-oxoguanine. These results indicate that the monomer can bind the maximum amount of 100% of the DNA (arrow B). At high protein concentrations a putative p50BD dimer is at a still higher molecular weight (DNA-p50BD$_2$) and this second band appears (Figure 2.11, arrow C). As the amount of protein is increased, the putative dimer begins to bind the 22G2 κB

DNA and the amount of DNA bound by the monomer begins to decrease (Figure 2.11, lanes 6-9, see arrows B and C).

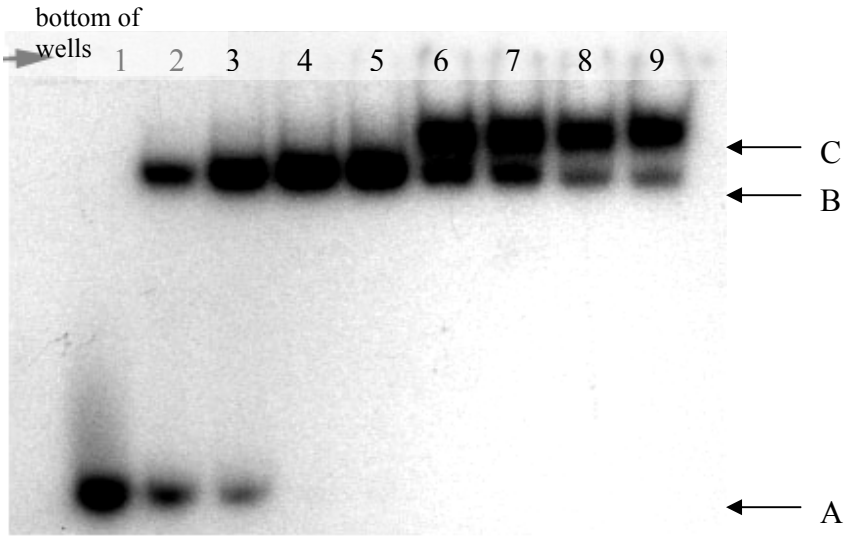

Figure 2.11: 22G2 κB DNA with p50BD.
Lanes 1-9: dsDNA + p50BD (0, 0.471, 0.942, 1.414, 1.885, 2.356, 2.827, 3.298, and 3.769 μM protein).

Interaction of the 22-mer κB modified at G3 DNA sequence with p50BD:

Only one faint binding band is observed (Figure 2.12) when p50BD protein is incubated with a 22-mer κB sequence modified in the G3 position with an 8-oxoguanine. These results indicate that the p50BD can only bind a limited amount of κB DNA with an 8-oxoguanine in the G3 position (Figure 2.12, see arrow B). A large residual amount of unbound DNA remains (lanes 4-9, arrow A).

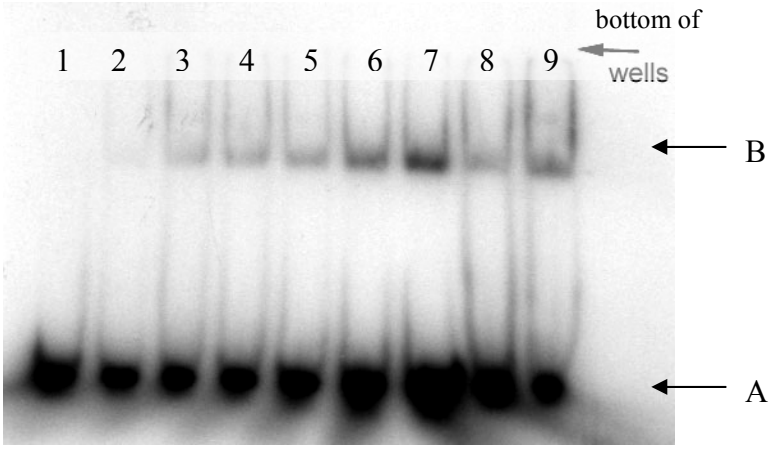

Figure 2.12: 22G3 with p50BD.
Lanes 1-9: dsDNA + p50BD (0, 0.471, 0.942, 1.414, 1.885, 2.356, 2.827, 3.298, and 3.769 μM protein)

Interaction of the 22-mer κB modified at G4 DNA sequence with p50BD:

8-oxoguanine modified at position G4 binds p50BD protein in a similar manner to the above gels with p50BD and κB DNA (Figure 2.9-2.12); unlike the 22-mer G2 (Figure 2.11), there is only one binding band is clearly observed (Figure 2.13), but it is possible that an unresolved second band for the dimer exists in lanes 7-10. These results indicate that the p50BD binds κB DNA with an 8-oxoguanine in the G4 position with an affinity close to that of unmodified DNA (Figure 2.13, arrow B). A small residual amount of unbound DNA remains (lanes 4-9, arrow A). For the densitometry analysis, the amount of protein required for each shift of DNA was divided in half as the concentration of DNA was 2x (or 0.52 μM). It was assumed that twice as much protein was required for twice as much DNA, thus for half the amount of DNA (0.26 μM) only half the amount of protein would be required to create the same DNA shifts.

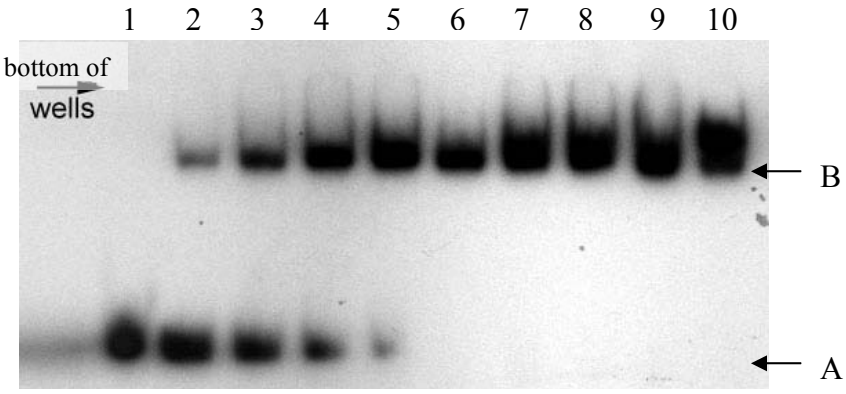

Figure 2.13: 22G4 with p50BD.
Lanes 1-10: dsDNA (concentration is 2x, 0.52 μM) + p50BD (0, 0.471, 0.942, 1.414, 1.885, 2.356, 2.827, 3.298, 3.769 and 7.068 μM protein)

Table 2.3: Densitometry for 22-mer κB sequences and p50BD

	% of DNA shifted by p50BD				
p50BD (μM)	**Control**	**8-oxoG1**	**8-oxoG2**	**8-oxoG3**	**8-oxoG4**
0	2.208424	1.060578	2.955006	0.732107	1.577256
0.236					21.78485
0.471	36.58448	4.076286	57.51619	4.303915	47.78349
0.707					72.54122
0.942	83.29771	23.92229	83.51295	11.83553	91.22873
1.178					99.82418
1.414	91.06419	23.92229	99.06544	13.11185	
1.885		52.26755		12.27109	
2.356		52.26755		14.74826	
2.827		57.80033		14.90688	
3.298		60.45242		12.75896	
3.769		90.70031		22.96632	
4.241		100			

Lane 1 corresponds to zero μM p50BD protein on the gels shown from Figure 2.9 to Figure 2.13; the pattern was that lane 2 up to lane 10 increased in increments of ~ 0.471 μM (200 ng) p50BD protein. The analyses of the densitometries for only Figure 2.9 were rounded up to the nearest hundred of ng of protein for K_{app} analysis which changed the μM concentrations; for example 194 ng protein became 200 ng (0.457 μM → 0.471 μM), and 388 ng became 400 ng (0.914 μM → 0.942 μM), and 582 ng became 600 ng (1.371 μM → 1.414 μM). The analysis of Figure 2.13 assumes that twice the concentration of modified DNA requires twice the concentration of protein to elicit the shifts. For the K_{app} calculations and Table 2.3, the values for the protein concentrations are divided in half and reported in μM values.

Interaction of the 30-mer κB DNA control oligonucleotide sequence with p50BD:

For Figure 2.14, a greater than 90% shift of the DNA is accomplished using 0.457 μM p50BD protein (lane 3 as compared to zero shift from lane 1, no protein) and a complete shift with 0.914 μM protein (lane 4). These concentrations of protein required to shift similar amounts of 22-mer κB DNA are exactly the same; 0.914 μM protein are required to have a 100% shift for the 22-mer control (Figure 2.9, lane 3). However, in no situation with the 30-mer κB DNA was there ever a second DNA shift due to monomeric and dimeric protein binding interactions. Excess protein confirms the 100% shift of 0.914 μM p50BD (lanes 4 – 7).

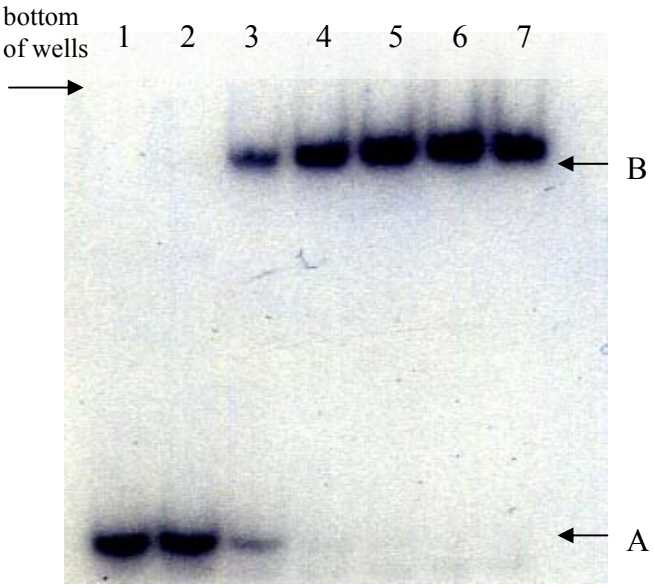

Figure 2.14: 30-mer control κB DNA and p50BD.
Lanes 1-7: dsDNA + p50BD (0, 0.229, 0.457, 0.914, 1.371, 1.828, and 2.285 μM protein).

Interaction of the 30-mer κB DNA modified at guanine positions G1, G2, and G3 sequences with p50BD:

The side-by-side comparison shows that the presence and location of the 8-oxoguanine modification completely determines the p50BD protein apparent binding

affinity (Figure 2.15). This figure shows clearly that 30-mer G3 modification has the poorest binding compared to the 30-mer control, G1, and G2 modified DNA.

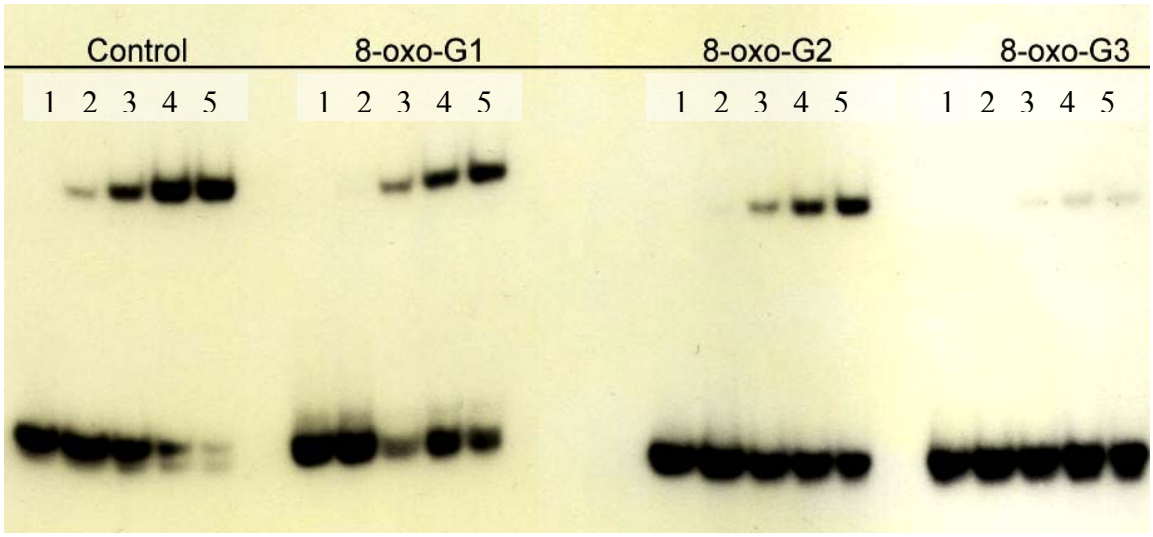

Figure 2.15: 30-mer dsDNA (all 2.6 μM); Control, 8-oxo G1, G2, & G3 with p50BD Lanes 1-5: 0, 0.457, 0.914, 1.371, and 1.828 μM p50BD.

The 22-mer 8-oxoguanine modified at position G2 κB DNA showed monomeric p50BD protein binding at 100% and then dimeric protein binding at higher concentrations of protein (2.356 μM protein, lane 6, Figure 2.11). Figure 2.15 for 8-oxoguanine 30-mer modified at position G2 does not include a lane of 2.356 μM protein, the highest amount of protein used was 1.828 μM; it is possible that a higher concentration of protein (~2.356 μM) could elicit a dual banding of dimeric and monomeric protein. It is feasible that the flanking regions of the oligonucleotide for the 22-mer as compared to the 30-mer influence the binding specificities for monomer versus dimer for modified κB DNA.

Table 2.4: Densitometry for 30-mer κB sequences and p50BD

	% of DNA shifted by p50BD			
p50BD (μM)	30-mer control	30-mer G1	30-mer G2	30-mer G3
0	0	0	0	0
0.457	59.4802	1.0042	1.07666	0
0.914	99	29.413	9.95949	2.0361
1.371	99.9	31.989	22.8742	3.1557
1.828		53.371	35.5561	3.4296

p50BD protein-free sample corresponded to lane 1 on the gels shown in Figure 2.14 and Figure 2.15; the pattern followed that lane 2 up to lane 10 increased in increments of 0.457 μM p50BD protein, such that lane 2 was 0.457 μM, lane 3 was 0.914 μM and so forth as indicated in the figure legends.

Interaction of the 30-mer κB DNA sequences with p50H67A, mutant protein:

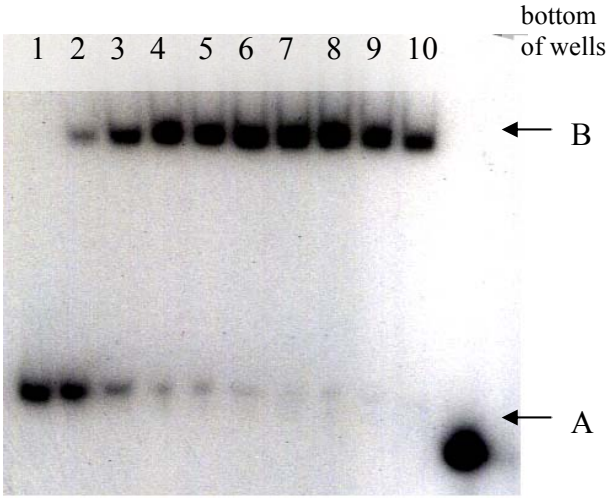

Figure 2.16: 30-mer control κB DNA and p50H67A.
Lanes 1-10: DNA (0.26 μM) + p50H67A (0, 0.457, 0.914, 1.371, 1.828, 2.285, 2.742, 3.199, 3.656, and 4.11 μM protein).
Lane 12: single stranded control DNA, 2x concentration (0.56 μM).

The mutant p50 protein, p50H67A, was incubated with 30-mer κB DNA sequences. A nearly 100% shift of the DNA is accomplished using 2.356 μM p50BD protein (lane 6) as evaluated by K_{app} (Table 2.5, page 46). Indeed, a 2.5-fold increase is required in p50H67A protein amount as compared to p50BD protein to fully shift all DNA (compare Figure 2.14 to 2.16).

Interaction of the 30-mer κB DNA sequence modified at position G1 with p50H67A:

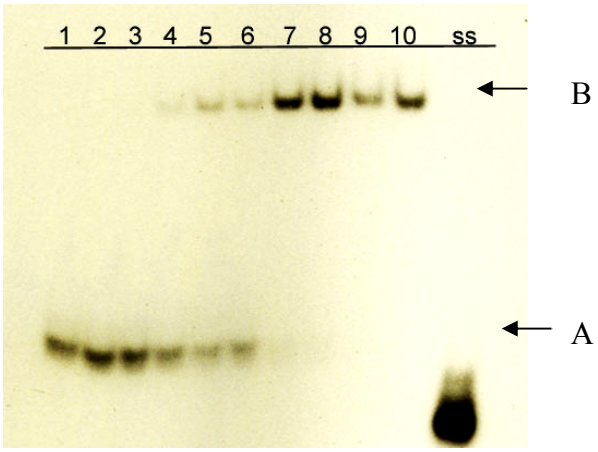

Figure 2.17: 30-mer G1 κB DNA and p50H67A.
Lanes 1-10: dsDNA (0.26 μM) + p50H67A (0, 0.457, 0.914, 1.371, 1.828, 2.285, 2.742, 3.199, 3.656, and 4.11 μM protein)
Lane 12: single stranded control DNA, 2x concentration (0.56 μM)

Gel shifts of the 8-oxoguanine modification at G1 for the 30 base pair oligomer Figure 2.17 shows that the protein binds better to the control strand than to the modified strands. There appears to be nearly a 100% gelshift by 2.827 μM p50H67A incubated with G1 modified 30-mer compared to 2.356 μM protein required to shift unmodified 30-mer DNA. Table 2.5 indicates that the binding of p50H67A is slightly worse for the G1 8-oxoguanine modified than that for the 30-mer control DNA.

If the histidine in position 67 is critical for binding class I κB DNA sites, a difference in binding affinity should be observed between the 30-mer control with p50BD and p50H67A (see Figures 2.14 and 2.15). The difference in binding affinity was around 2.5-fold, which seems indicative of a role for histidine 67 in binding to the consensus sequence. The mutant was not pursued further; the results indicated that the importance of the mutation, shown in terms of binding affinity, was not as dramatic as it would have

been if the histidine position at 67 was critical for making bonds to non-modified and modified κB DNA.

Table 2.5: Densitometry for 30-mer κB sequences and mutant p50H67A

		% of DNA shifted by p50BD	
lane	p50H67A (μM)	control	8-oxoG1
1	0	2.6224	0
2	0.457	29.1754	0
3	0.914	67.3939	0
4	1.371	87.2181	14.3406
5	1.828	87.9168	35.6470
6	2.285	99	35.6470
7	2.742	99	99

From Table 2.5, zero μM p50H67A protein corresponded to lane 1 on the gels shown in Figure 2.16 and Figure 2.17; the pattern followed that lane 2 up to lane 10 increased in increments of 0.457 μM p50BD protein, such that lane 2 was 0.457 μM, lane 3 was 0.914 μM and so forth as indicated by the figure legends.

The NF-κB proteins are flexible in their binding; this is demonstrated by the mutant p50H67A protein, which was capable of binding the κB DNA consensus site. Nonetheless, it is known that these small differences in binding affinities for κB sequences can have an impact on the expression of genes. Perhaps the importance of the different binding affinities can only be seen *in vivo*. This leaves the door open to the possibility that the role of the DNA sequence, any modifications, and DNA conformation has an important regulatory responsibility in gene expression with the NF-κB protein

Discussion:

The p50 binding domain, residues 23 to 366, and a single amino acid mutation of histidine 67 to alanine 67 were cloned as an N-terminal his_6-tagged protein. These proteins were expressed and purified as active proteins.

The effect of 8-oxoguanine at each guanine site in the consensus sequence of κB DNA on the binding affinity of p50BD was determined on a 22-mer and a 30-mer double-stranded DNA oligonucleotide containing the NF-κB binding site with modifications at guanine sites (Figure 2.9 – Figure 2.13). The addition of a carboxyl moiety at position 8 on guanine (creating 8-oxoguanine) changes the binding affinity for the κB sequence. It has been seen that the non-modified control binds the p50 binding domain homodimer better than certain 8-oxoguanine modified κB DNA at specific sequences. Both 8-oxoguanines G2 and G4 modified DNA binds with an affinity better than that of non-modified control κB DNA. The 8-oxoguanine G2 has an interesting binding pattern with the presence of dual binding bands (Figure 2.11) which indicates that monomeric p50BD binds initially, and that at higher protein concentrations, the p50BD dimer can bind. It has been proposed that the loss of a hydrogen bond donor-acceptor pair from the arginine R59 of p50BD to the N7 (modified) of 8-oxoguanine G2 accounts for the loss of the p50 binding affinity (see Figure 2.2, page 23).

Earlier work investigated the apparent dissociation constants (K_{app}, Table 2.6, p49) of a full length dimeric p50 protein (Promega) with 8-oxoguanine modified κB sites. From the early work, the relative K_{app} for the unmodified control was found to be 0.672 μM with little change in the 50% binding affinity observed with the 8-oxoguanine modifications at G2 and G4 for the 22-mer. Additionally, the 8-oxoguanine modification

at G3, showed a nearly 4-fold decrease in K_{app} for binding of the p50 subunit to this modified DNA sequence versus the unmodified DNA sequence. Earlier work with 8-oxoguanine G3 modified κB DNA and lowered p50 binding affinity suggested that this modification can cause recognition loss of one of the κB DNA half sites.[9] This relationship appears to be true for the truncated p50 monomeric protein, p50BD, as well.

DNA-p50BD protein interactions

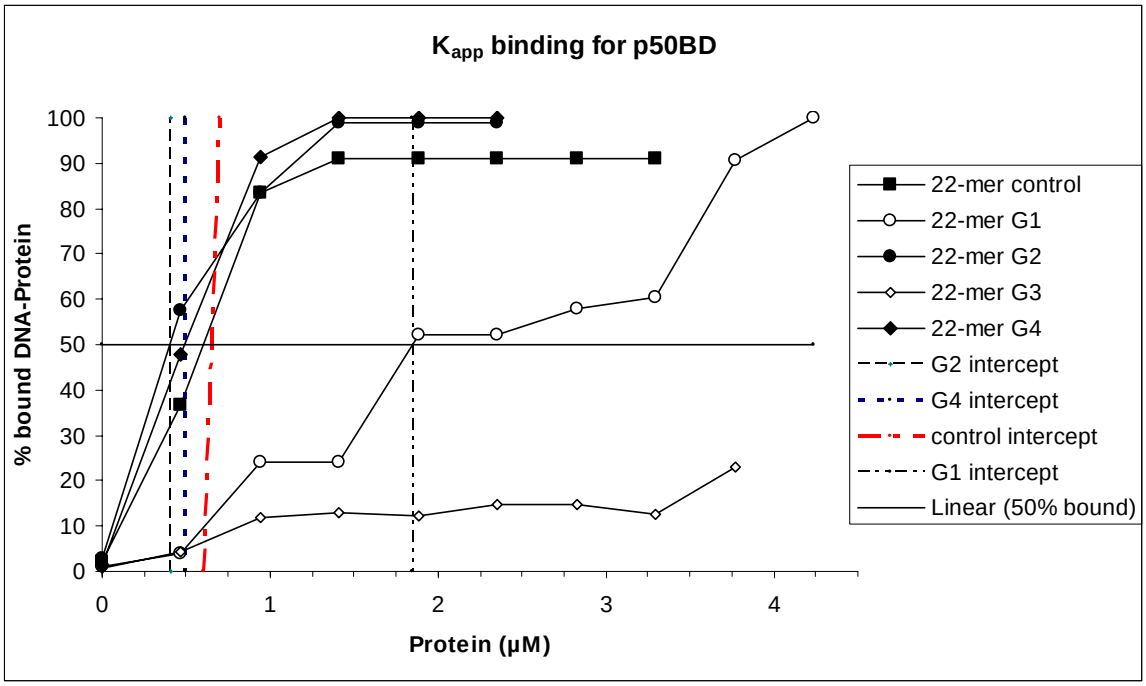

Figure 2.18: Data taken from **Table 2.3**. K_{app} binding for 22-mer κB DNA oligonucleotide sequences and p50BD. There are no error bars as the one gel considered the 'best' of each sequence was analyzed by densitometry.

It was found that the clone p50BD protein behaved in a manner analogous to the full length Promega p50 protein with the same oligomer sequences, with the exception of the 22-mer modified at G1. In fact, the p50 binding domain-only protein had apparent binding affinity of 0.605 μM compared to the binding affinity of 0.672 μM for full-length dimer protein (see **Table 2.6**) for control κB DNA. With modified κB DNA sequences,

the *truncated monomeric* p50 protein, p50BD, retains the ability to interact in a manner similar to the *full-length dimeric* p50 protein. The fewer number base pairs in the engineered protein (consisting of the binding domain only), consequently results in fewer potentially stabilizing amino acid residues. However, the lack of a few amino acid residues apparently does not greatly impact the protein's stability upon binding κB DNA.

Table 2.6: Binding affinities of the 22-mer control and 8-oxoguanine modified DNA with p50 binding domain and p50 (whole protein). p50 data taken from Hailer-Morrison, et al (2003) *Biochem.* **42**, 9761-9770.[9]

Oligonucleotide	p50 binding domain only K_{app} binding affinity (μM)*	p50 (Promega, dimer) K_{app} binding affinity (μM)*
Control	0.605	0.672 +/- 22
8-oxo-dG at G1	1.849	0.283 +/- 7
8-oxo-dG at G2	0.405	0.644 +/-35
8-oxo-dG at G3	10.69	2.340 +/- 40
8-oxo-dG at G4	0.498	0.550 +/- 35

* The K_{app} for the non-modified control and 8-oxoguanine modified oligonucleotides were determined graphically as the point where the percent bound was 50%.

For binding affinity, a lower number indicates a better binding of protein to DNA, and a higher number indicates a poor affinity of protein for DNA. The binding affinities above in the column "p50 binding domain only" were calculated assuming that the molar ratio of dsDNA to protein was 1 to 1 as compared to the earlier work with dsDNA to full-length p50 protein ratio at 1 to 2. For half-site binding, when comparing the 22-mer control DNA binding with p50BD to the binding of modified oligonucleotides with p50BD, it was seen that the binding affinity was best for the 8-oxoguanine modified at G2, then G4, and then followed closely by the control DNA. When comparing p50BD protein binding to control κB DNA (Figure 2.9, K_{app} = 0.605 μM) with p50BD with 22G1 modified κB DNA (Figure 2.10, K_{app} = 1.849 μM) it is seen that the truncated p50BD protein has a poorer affinity for modified DNA at the G1 position. This result is in direct

contrast to that of the whole p50 protein; 8-oxoguanine modified at G1 had a better binding affinity (0.283 μM) than control DNA (0.672 μM) for the Promega p50 dimer.

The EMSA for 22G2 showed two DNA-protein binding bands with a higher concentration of protein (Figure 2.11) due to the p50BD binding as either a monomer or a dimer to the κB DNA. The results indicate that the protein binds independently as a monomer for lower p50BD—DNA concentrations (Figure 2.11, arrow B) however, given enough p50BD protein, ~ 2.356 μM, the 22-mer 8-oxoguanine G2 modified DNA will be bound at both κB sites with two p50BD monomers – giving a dimer protein (see arrow C, Figure 2.11). A 100% shift was observed with the putative monomeric protein. Integration was based on arrow B, the monomer; further calculations for higher protein concentration integration involved the addition of the two shifted bands (arrow B and C, Figure 2.11). Work with the whole protein indicated no such dual banding with 8-oxoguanine modified at G2, however the concentration of protein was 2 μM or less, which is perhaps not enough protein to cause a dual banding.

The EMSA for the 22G3 showed that the modification negatively impacts DNA binding, with an extrapolated by linear regression K_{app} of 10.69 μM (Figure 2.12). This loss of binding, reflected in a higher K_{app} values, was proposed to be due to loss of the half site of the κB DNA. The greatest percentage of protein bound to DNA was determined to be 23%, thus the K_{app} at 50% bound DNA-protein was never achieved and was extrapolated graphically (50% bound DNA-protein = 4.318603143x + 3.820307386, where x = K_{app} (μM)). The poor binding with 8-oxoguanine modified at G3 is in agreement with the trend seen with whole p50 protein.

Comparing the 22-mer modified G4 (Figure 2.13) to control κB DNA (Figure 2.9), it was observed that the modified κB DNA requires less p50BD protein to exact a complete shift. This is based on the assumption that twice the concentration of DNA requires twice the concentration of protein to gel shift. The K_{app} values were quite close for binding affinities for the G4 and the control; more gels evaluated by densitometry could possibly determine if this relationship is valid and that there is a slight but distinct difference between the two oligonucleotide sequences.

Taken as a whole, these results indicate that the recognition of κB DNA by p50BD decreases with 8-oxoguanine modification except for at the G2 and G4 positions. Furthermore the loss in binding affinity is most dramatically seen with modification at G3. The 8-oxoguanine modification has the least amount of impact with modifications at G4 having a K_{app} similar to the K_{app} for control. The most interesting interactions between DNA and protein are seen with the 8-oxoguanine G2 modification where the protein can be visualized binding as both a monomer (Figure 2.11, arrow B) and as a dimer (arrow C).

DNA-p50H67A (mutant protein) interactions

The binding of p50H67A with 30-mer κB control DNA was performed to determine the importance of the histidine in position 67 of the human p50 protein. A difference was observed between the binding of p50BD protein and p50H67A protein to κB DNA (see Figures 2.14 and 2.16); the p50BD has greater affinity for the 30-mer control sequence and the 8-oxoguanine modified G1 sequence than the p50H67A (K_{app}p50BD = 0.386 μM versus K_{app}p50H67A = 0.707 μM for control κB DNA). The

histidine in p50BD protein makes potential contacts with the G_1 which accounts for the difference in binding of 1.755 μM versus 2.391 μM when comparing p50BD and p50H67A binding to 8-oxoguanine modified at position G1. The histidine to alanine mutation allows the p50H67A protein to mimic the p65 (RelA) protein, which prefers a 9 base pair sequence. The anticipated result was that the mutant p50H67A would not bind the 30-mer κB DNA sequence or would bind extremely poorly and would be reflected in a high numeric value for the K_{app}. Thus the slightly diminished binding affinity was not significant enough to confirm that the histidine (H67) is critical for binding modified κB oligonucleotides. Perhaps the binding affinity would be significant *in vivo*.

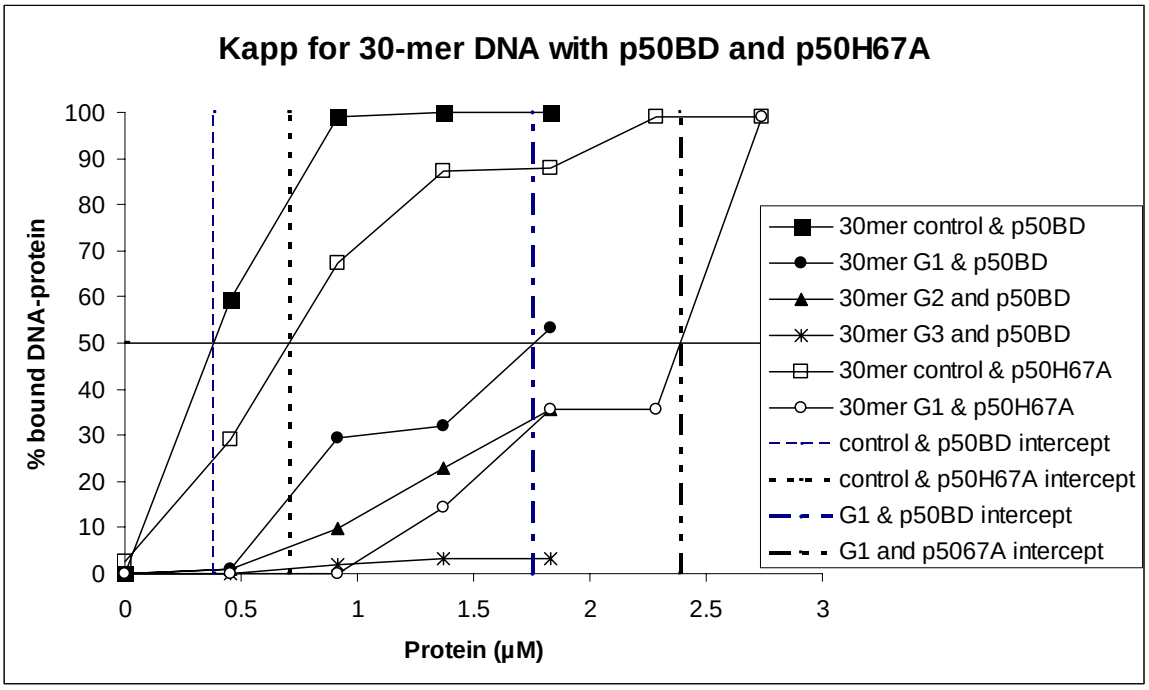

Figure 2.19: Data taken from **Table 2.4** and **Table 2.5;** K_{app} for 30-mer κB DNA oligonucleotide sequences with p50BD or p50H67A. No error bars were included as only the one best gel of each sequence was analyzed by densitometry.

Table 2.7: Binding affinities of 30-mer control and 8-oxoguanine modified DNA with p50BD (binding domain) and p50H67A (mutant)

P50BD		P50H67A	
Oligonucleotide	K_{app} binding affinity (μM)*	Oligonucleotide	K_{app} binding affinity (μM)*
Control	0.386	Control	0.707
8-oxo-dG at G1	1.755	8-oxo-dG at G1	2.391
8-oxo-dG at G2	2.690	8-oxo-dG at G2	n/d
8-oxo-dG at G3	22.94	8-oxo-dG at G3	n/d

* The K_{app} for the non-modified control and 8-oxoguanine G1 modified oligonucleotides were determined graphically as the point where the percent bound was 50%. The K_{app} for the 8-oxoguanine modifications to G2 and G3 bound with p50BD were extrapolated by linear regression. n/d indicates that the relationship was not determined.

The p50H67A was also able to bind the 30-mer κB DNA 8-oxoguanine modified at position G1. It was predicted that the 8-oxoguanine containing DNA modified at G1 would bind the mutant protein differently as compared to the unmodified κB DNA. 8-oxoguanine, with its increased number of donor/acceptor contacts (see Figure 1.3 A & B, page 7) could potentially stabilize protein bonding to DNA modified at position G1 by hydrogen bond/electrostatic contacts to the mutant protein. The possible areas for contact include the carboxyl moiety of the protein backbone from alanine 67 to glycine 68 as a hydrogen bond acceptor from the hydrogen of N7 of 8-oxoguanine and arginine 59 NH_2 as hydrogen bond donor to the carboxy at C8 of 8-oxoguanine. The values for the mutant protein binding to 8-oxoguanine G1 were expected to have lower K_{app} values indicating a greater binding affinity as compared to the K_{app} values for 8-oxoguanine binding to p50BD. This predicted relationship was not observed, and it is possible that the 8-oxoguanine at G1 does not make the predicted contacts to protein to stabilize binding. A crystal structure of the mutant protein bound to κB DNA (non-modified and modified) would clarify the DNA-protein interactions.

It was seen that the binding affinity for the p50BD versus p50H67A in binding to control κB DNA was around 2 -fold difference. Taking all the information together, these results suggest that the histidine H67 is important in binding class I κB DNA. While conserved for this consensus sequence, this amino acid is not shown to be critical for binding a small oligonucleotide sequence, as there is a level of binding visible (Figure 2.16 versus Figure 2.14). This could be the result of the inherent flexibility of the protein which still allows for DNA binding even if the sequence is not ideal (containing the class I κB site of 5'-GGG RN-3' half-site, where R is purine and N is any nucleotide). Comparing the 8-oxoguanine modifications made to κB DNA and control κB DNA, the results indicate that the p50BD protein binds better to non-modified DNA and perhaps modifications to DNA by an oxidative mechanism is not necessarily a secondary form of transcriptional regulation in the genome. Clarifications to this theory could be determined by using a histone-wrapped full length gene with this exact consensus sequence κB DNA to mimic *in vivo* DNA-protein actions. It is possible that the DNA-wrapped histone confers protective shielding to sites on DNA susceptible damage and/or protein binding.

[1] Sen, R. and Baltimore, D. (1986) Multiple nuclear factors interact with the immunoglobulin enhancer sequences. *Cell* **46**(5), 705-716.

[2] Aggarwal, B.B. (2004) Nuclear factor-κB: The enemy within. *Cancer Cell* **6**, 203-208.

[3] Baldwin, A. S. (1996) The NF-κB and IκB proteins: new discoveries and insights. *Annu. Rev. Immunol*. **14**, 649-681.

[4] Chytil, M. and Verdine, G.L. (1996) The Rel family of eukaryotic transcription factors. *Curr. Opin. Struct. Biol.* **6**(1): 91-100.

[5] Huang, D.-B., Phelps, C.B., Fusco, A.J., and Ghosh, G. (2005) Crystal structure of a free κB DNA: insights into DNA recognition by transcription factor NF-κB. *J. Mol. Biol.* **346**: 147-160.

[6] Ghosh, G., Van Duyne, G., Ghosh, S., and Sigler, P.B. (1995) Structure of NF-κB p50 homodimer bound to a κB site. *Nature* **373**, 303-310.

[7] Müller, C.W., Rey, F.A., Sodeoka, M., Verdine, G.L., and Harrison, S.C. (1995) Structure of the NF-κB p50 homodimer bound to DNA. *Nature* **373**, 311-317.

[8] Gilmore, T.D., Koedood, M., Piffat, K.A., and White, D.W. (1996) Rel/NF-κB/IκB proteins and cancer. *Oncogene* **13**, 1367-1378.

[9] Hailer-Morrison, M.K., Kotler, J.M., Martin, B.D., and Sugden, K.D. (2003) Oxidized guanine lesions as modulators of gene transcription. Altered p50 binding affinity and repair shielding by 7,8-dihydro-8-oxo-2'-deoxyguanosine lesions in the NF-κB promoter element. *Biochemistry* **42**, 9761-9770.

[10] Glover, D.M. DNA cloning: a practical approach, Volume 1 1985, Oxford: IRL Press.

CHAPTER 3

DNA-protein with chromium exposure could lead to crosslinking:

Background on previous work:

The five different κB DNA sequences, non-modified and modified at guanine positions, for the 22-mer, 5'-AGT TGA **$G_1G_2G_3$ G_4AC TTT CC**C AGC C-3', have been shown to have discrete binding affinities for the p50 binding domain protein and p50H67A protein. The 30-mer oligomer sequence, 5'- TCC GCT **$G_1G_2G_3$ G_4AC TTT CC**G CGG AGA CTC TAG-3', contains a slightly different flanking regions, however the consensus sequence (bold) remains the same. These oligonucleotide κB DNA sequences of 22 and 30 base pairs were used to explore the complex interactions of oxidized DNA and p50BD protein with chromium treatment.

Previous work has established that, by reduction and oxidation potentials, it is energetically favorable to further oxidize 8-oxoguanine-modified DNA while reducing chromium(VI) if the two species are together in solution. If water acts as a nucleophile, an additional oxidative event generates guanidinohydantoin (Gh) and spiroiminodihydantoin (Sp) (see Figure 1.5, page 9). When protein is bound to modified DNA it can potentially exclude or out-compete the water. Thus while chromium is reduced in an oxidative event, and protein acts as a nucleophile, the oxidation of DNA could crosslink the DNA—protein together in a covalent bond. This covalent crosslinking of DNA and protein would establish a new mode of chromium toxicity with damaged DNA.

Amino acids of interest in forming covalent bonds with any of the four different 8-oxoguanine modified bases in the κB DNA oligonucleotide are at the consensus site of

the p50BD protein; these include arginine 57, arginine 59, tyrosine 60, histidine 67, glutamate 60, and lysine 244 (Figure 3.1, taken from Huang et al., and 1SVC from the Protein Data Bank; murine p50 - amino acids relative positions are three less base pairs compared to human p50).[1]

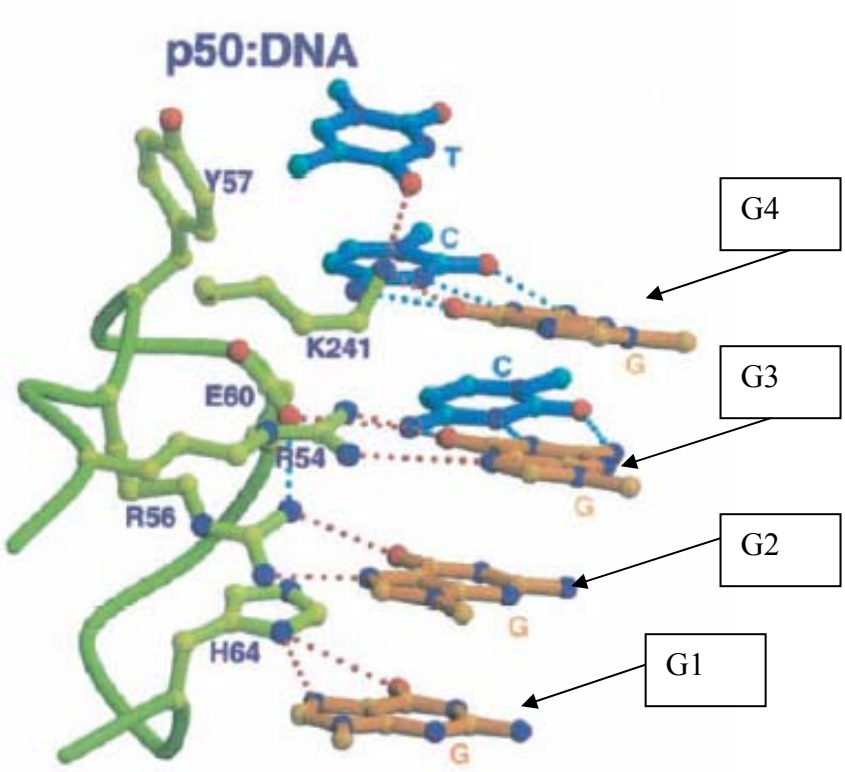

Figure 3.1: Half site binding of p50 with DNA (4 guanine sequence)
Taken from Huang, et al. (2003) *Proc. Natl. Acad. Sci.* **100**, 9268-9273.[2,3]

The potential areas of binding include, but are not limited to the G_1 of κB DNA with histidine 67 (H64) of p50BD protein and G_4 of κB DNA with lysine 244 (K241) of p50BD protein (Figure 3.1). The functional group of histidine is the imidazolium moiety, with two nitrogens available for chemical interactions. Histidine has a $pK_a = 6.0$, which means that at pH 6.0 half of the molecules are charged, and histidine is neutral on the basic edge of physiological pH range, 6.5 to 7.6.[4, 5] Thus histidine often contributes

hydrogen bonds in enzymatic reactions. The lysine is available to form a Schiff base through the distal amine depending on solution conditions. At physiological pH it is positively charged with a $pK_a = 10.54$. The arginines, with their available nitrogen groups, are in close proximity to guanines 2 and 3 (G2 and G3, Figure 3.1). These amino acids are also able to form Schiff base bonds with the $pK_a = 12.48$ for the guanidinium moiety.[4]

The amino acids listed above have the potential to act as nucleophiles on 8-oxoguanine modified DNA competing with water which is a relatively poor nucleophile. The nucleophile can attack the C5 position on the guanine (see Figure 2.2, page 23) and attach to the nucleic acid moiety.

Materials and methods:

Deoxyribonucleotides. Unmodified oligonucleotides with the κB consensus sequence were obtained from IDT DNA (Coralville, IA). Modified 22-mer DNA sequences containing an 8-oxoguanine in the NF-κB protein p50 homodimer consensus sequence (5'-AGT TGA **$G_1G_2G_3$ G_4AC TTT CC**C AGC C-3', where the bold bases indicate the consensus sequence and the G_{1-4} indicate positions of 8-oxoguanines in the recognition sequence) were obtained from TriLink Biotechnologies (San Diego, CA). Modified 30-mer DNA sequences containing the sequence 5'- TCC GCT **$G_1G_2G_3$ G_4AC TTT CC**G CGG AGA CTC TAG -3' (again the bold bases indicate the consensus sequence and the G_{1-4} indicates positions of 8-oxoguanines in the recognition sequence) were also obtained from TriLink Biotechnologies. HPLC purification of the 22-mer oligonucleotide strands was performed using a Dionex DNAPac PA-100, 4 mm x 250 mm anion exchange column. Elution was accomplished with a linear gradient of 90% mobile phase A (10% aqueous acetonitrile) and 10% mobile phase B (1.5 M ammonium acetate (pH 6.2), 10% acetonitrile) to 100% mobile phase B over the course of 22 minutes. The 30-mer oligonucleotide was purified in a similar manner, however mobile phase A also contained 500 mM NaCl and elution was accomplished with a linear gradient of 90% A and 10% B to 100% mobile phase B over 30 minutes. Column elutions of oligonucleotides were observed by diode array at 268 nm. The single-peak elution of oligomer was evaporated to remove the volatile acetonitrile, eluted through a BioRad chromatography column 6 and stored at -20˚C until needed for testing. The NaCl from the 30-mer oligonucleotides was removed by elution through a BioRad chromatography column 30. Standard methods were employed to 5'- ^{32}P end-label specific oligomers. The control or 8-

oxoguanine containing single stranded DNA was incubated with polynucleotide kinase and 10 μCi of ^{32}P-γ-ATP for 30 minutes. Column elutions with a Micro Bio-Spin 6 chromatography column from BioRad (Hercules, CA) removed the enzyme and unincorporated nucleotides. The radiolabeled single stranded DNA was annealed to complement DNA by heating to 95˚C and slowly cooling 1˚C / 1 minute using a Peltier Thermal Cycler from MJ Research (BioRad, Waltham, MA).

NF-κB p50BD Transcription Factor Protein. The p50 binding domain sequence from residues 23 to 366 was created as described in chapter 2 by cloning into the pPROEX HTa II plasmid to give the protein as an N-terminal His_6-tagged protein.

Protein purification. The expression plasmids, in BL21 (DE3) cells, were grown to an OD_{600} of 0.3-0.6 at 37˚C in LB media containing 25 μg/mL ampicillin, as the pPROEX HTa contains an ampicillin resistance cassette. Cells were induced with IPTG to a final concentration of 0.1 mM and incubated for 4 hours at 37˚C. Cells were then harvested by centrifugation at 4˚C and 5,000 rcf, and frozen at -20˚C for later use. After thawing on ice, cells were lysed using the BugBuster® protocol and reagent (Novagen, 5 mL reagent per gram wet cell paste), lysozyme (Sigma, 0.5 mg per gram wet cell paste), Benzonase nuclease (Novagen, 1 μL per mL BugBuster® reagent), and protease inhibitor cocktail (Roche, 1 tablet dissolved in 2 mL H_2O, use 0.2 mL per 5 mL extraction reagent). Cell lysate was filtered through a Ni-NTA column (Qiagen). Protein was washed with Solution A and B (50 mM NaH_2PO_4, 300 mM NaCl, with 10 mM and 20 mM imidazole respectively) and eluted with Solution C (50 mM NaH_2PO_4, 300 mM NaCl, 250 mM imidazole). The elution fraction was de-salted using a Microcon YM-10 and eluted into protein storage buffer (20 mM HEPES, 50 mM NaCl, pH 7). An aliquot was reserved for

BCA protein concentration analysis (BCA kit, Pierce, Rockford, IL), and the remaining sample was diluted in half with protein storage buffer containing 40% glycerol, aliquoted into sub-samples, and stored at -80˚C.

Chromium(V)-Salen. Three mg chromium(III)-Salen were dissolved in 300 µL dry acetonitrile (20 mM chromium(III)-Salen). Three mg iodosyl benzene were added to the solution and incubated for 30 minutes. The solution (chromium(V)-Salen) was diluted to appropriate concentrations and used immediately.

HPLC shift Assay. DNA-protein binding reactions were performed using 50 µM 5'-DNA which had been annealed to its complement to create double stranded DNA (dsDNA) and approximately 32 µg p50BD protein. The reaction buffer for the DNA-protein binding was 5 µL Buffer A (20 mM HEPES, 50 mM NaCl, pH 7) and Buffer B (Promega: 20% glycerol, 5 mM $MgCl_2$, 2.5 mM EDTA, 2.5 mM DTT, 250 mM NaCl, 50 mM Tris-HCL, pH 7.5, 0.25 mg/ml poly(dI-dC)) to a total volume of 100 µL. The DNA and protein were allowed to react for 20 minutes before chromium(V)-Salen was added (at varying ratios to DNA, frequently 1:1,1:2, 1:5, 1:10, and 1:100) and incubated for 30 minutes at room temperature. A cation exchange column, engineered by glass pipette, glass wool, 15 mg CM-Sephadex C-25-120 Resin (Sigma), and 200 µl H_2O, removed the cationic chromium from the DNA-protein solution. The DNA-protein sample was dried to 15 µL for sample injection onto the HPLC. The concentrated sample was injected onto a Dionex DNAPac PA-100, 4 mm x 250 mm anion exchange column. Elution was accomplished with a linear gradient of 90% mobile phase A (10% aqueous acetonitrile) and 10% mobile phase B (1.5 M ammonium acetate (pH 6.2), 10% acetonitrile) to 100% mobile phase B over the course of 22 minutes. Later HPLC shift assays used only

reaction Buffer A with concentrated p50BD protein and DNA to a total volume of 10 μL after chromium(V)-Salen addition. The sample cleanup on the cation exchange column and HPLC sample injection was performed as described above.

Electromobility Shift Assay (EMSA or gelshift). DNA-protein binding reactions were performed using 2.6 μM 5'-^{32}P radioactive-labeled DNA which had been annealed to its complement to create double stranded DNA (dsDNA). The reaction buffer for the DNA-protein binding was 300 mM NaH_2PO_4. When carrying out an EMSA on a polyacrylamide gel; either a native 4% polyacrylamide gel was poured (with or without urea), or a 6% Invitrogen pre-poured DNA retardation gel was used. The denaturant used was 8 M urea added to the sample or added to the gel, heat, a combination of both. The DNA and protein were allowed to react for 20 minutes before running on the gel. Additionally, glycerol (1 μL, 40%) was added to all reaction mixes to increase density and help with sample loading. Unless a free well was available for dye only, the sample 'DNA only' was the only well to have loading dye added in order to minimize any interference of the dye with the DNA and protein binding interactions. The gels were run at 250-300 V for ~10 minutes. The gel shifts were analyzed by autoradiography (Kodak).

Analysis of Reductively-trapped Schiff Base complexes of hOGG1. The chromium(V)-Salen treated, ^{32}P-labeled dsDNA (2.6 μM) was incubated with hOGG1 (15 nM, New England Biolabs) in 10 μL reaction buffer (20 mM Tris-Cl (pH 8.0), 1 mM EDTA, 1 mM DTT, 100 μg/mL BSA, 3 μL H_2O) in the presence of 65 mM $NaCNBH_3$ at 37˚C for 60 minutes. Glycerol (1 μL, 40%) was added to the sample. The gel shifts was analyzed as described above. hOGG1 (38 KDa) is of comparable size to the p50BD protein (42.4

KDa) for comparison of crosslinking. Visualization of this reductively-trapped crosslink will indicate if it is possible to visualize oxidatively-trapped or crosslinked DNA-protein.

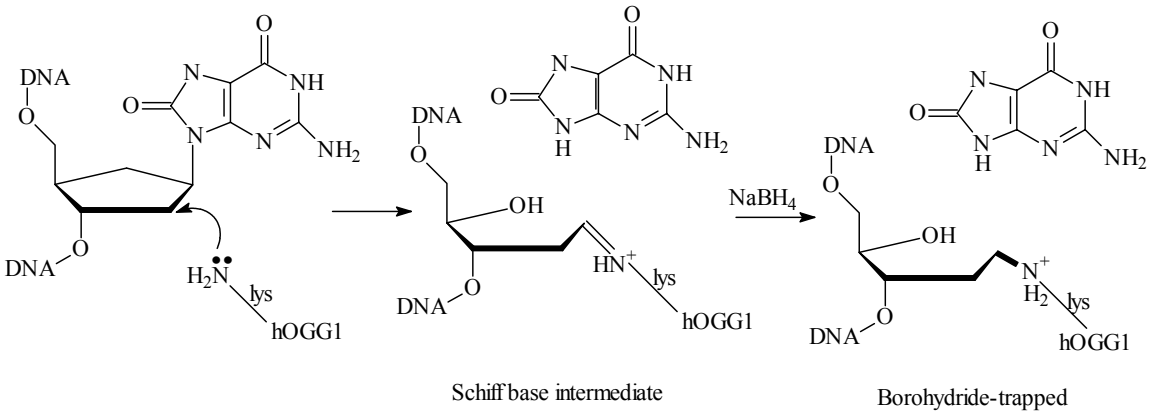

Figure 3.2: Borohydride trapping of lysine 249 on hOGG1

Results

Covalent bonds are more resistant to degradation, meaning heat, urea, or similar conditions that disrupt other bonds (ionic, van der Waals, or hydrogen bonds), and for observation by HPLC these covalently bonded moieties could elute later or travel on a PAGE gel as a single, larger complex than the DNA alone. An electrostatic bond of DNA--protein will not remain as a single peak in HPLC system nor as a single DNA-protein band under rigorous denaturing conditions in a gel system.

The HPLC purification provides an elegant method to separate forms of modified DNA. Modifications to DNA such as Gh and Sp can be resolved from 8-oxoguanine even at higher ratios of 1:100, DNA : chromium (Figure 3.3). Therefore modifications to DNA, such as a covalent protein linkage could also be resolved on HPLC as compared to an 8-oxoG modification.[6] Figure 3.3 shows Gh/Ia tautomers at peaks 1 and 2, the 8-oxoG at peak 3, peak 4 is Sp, and peak 5 is an unidentified further oxidized species.

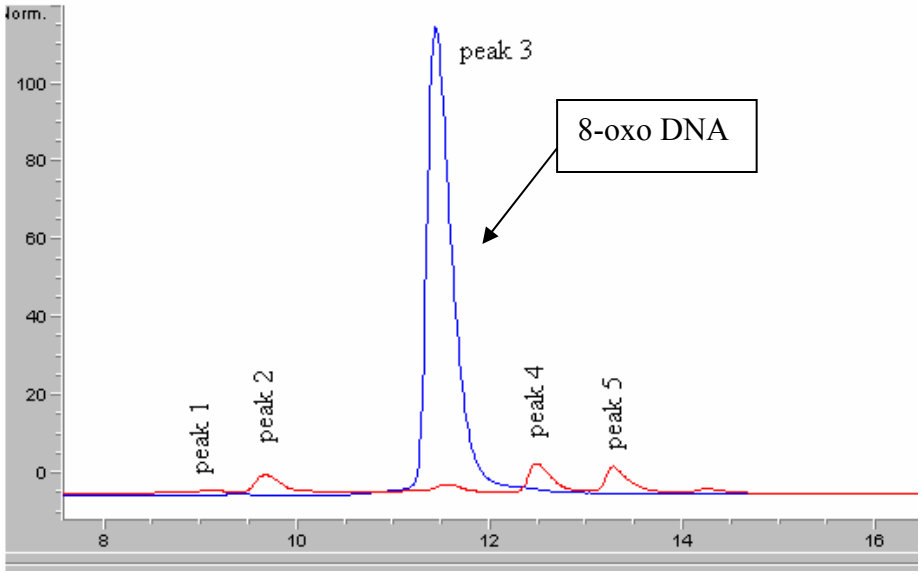

Figure 3.3: HPLC trace of water as nucleophile on 8-oxoguanine exposed to chromium
Trace Blue = 8-oxo DNA, Trace Red = Cr(V)-Salen treated 8-oxoguanine.
Peaks 1 & 2 – Gh/Ia, tautomers, Peak 3 – 8-oxoG, Peak 4 – Sp
Peak 5 – further oxidized 8-oxoG^{ox}, Gh^{ox} or Sp^{ox}, ratio of DNA to Chromium is 1:100.

In Figure 3.4, for the 'DNA + p50BD + chromium', the DNA was incubated with p50BD protein for 20 minutes before a 30 minute chromium(V)-Salen exposure. The electrostatically bonded 'DNA + p50BD' (red) looks very similar to the 'DNA + p50BD + chromium' (magenta); crosslinking would create a system resistant to degradation, and covalently bonded DNA–protein should elute at a different time than electrostatically bonded DNA--protein. Perhaps the p50BD protects the oxidized DNA from further oxidation or there was not enough protein to successfully bind and shift the DNA on the HPLC, or it was lost in the clean-up process. The trace of '8-oxo DNA + chromium' in Figure 3.4 (green) is the same sample composition as the '8-oxo DNA + chromium' from Figure 3.3 (red), however, the DNA:Cr ratio is 1:1, the peaks for Gh/Ia appear less resolved and no Sp peak is detected. A higher ratio of chromium, such as 1:2 DNA to chromium, would create more Gh/Ia and Sp for improved peak resolution. The DNA sample with protein and chromium is not distinctly different than the DNA + chromium sample, however, previous work at higher chromium concentrations indicated that the protein shields the DNA from chromium damage.[7] It is possible that the cation exchange column contributed to a small loss of DNA in samples placed on the HPLC. If a covalent crosslink had occurred and was detected by the HPLC, it is possible that the complexes' charge might be different thus there would be a DNA-p50BD complex eluting at a different time in the magenta trace, and this was not observed.

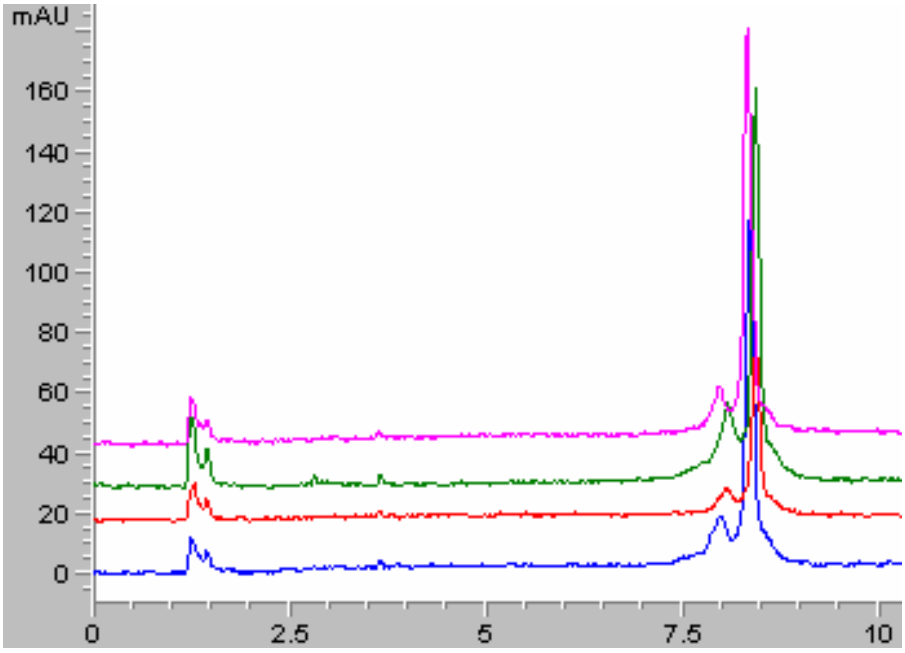

Figure 3.4: HPLC trace of 8-oxoguanine with and without protein, and with chromium
Controls: Blue-ds-8-oxoguanine DNA only; Red- 8-oxoguanine dsDNA + p50BD;
Green- 8-oxoguanine dsDNA + chromium; 8-oxoguanine DNA + p50BD;
Sample: Magenta- - 8-oxoguanine DNA + p50BD + chromium;
* Initial amounts of DNA were the same, HPLC traces are offset for comparison

It was determined that the HPLC, as set up with an anion exchange column, was not the optimal setting for determining covalent DNA-protein bonding. One system that required less DNA and less protein was a polyacrylamide gel using radiolabeled DNA. Electrophoretic gel shift assays of DNA-protein were performed to determine K_{app} values for binding affinities for the five 22-mer modified and unmodified κB DNA sequences (chapter 2).

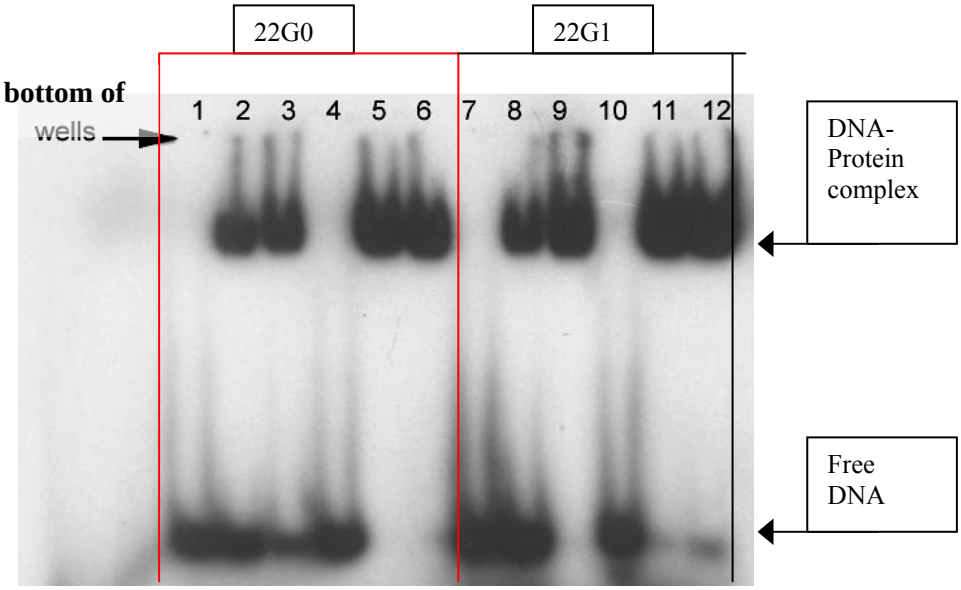

Figure 3.5: Gel comparison of control vs. 8-oxoG DNA with and without chromium
Lanes 1-6 unmodified DNA, Lanes 7-12 8-oxo G1 DNA
L→R the samples are DNA, DNA + protein, DNA + protein with urea, DNA + chromium, DNA + protein + chromium, and DNA + protein + chromium with urea.
*Denaturant (8 M urea) in lanes 3, 6, 9, and 12

In Figure 3.5, control DNA, 22G0, is in lanes 1-6 and 8-oxoG modified at position 1, 22G1, is in lanes 7-12; the protein is p50BD. The sample types are DNA (lanes 1, 7), DNA + p50BD (2, 8), DNA + p50BD denatured (3, 9), DNA + chromium (4, 10), DNA + p50BD + chromium (5, 11), and DNA + p50BD + chromium denatured (6, 12).

For the non-modified strand, if a covalent crosslink formed, it would show in lane 6 (Figure 3.5, DNA-Protein complex row) with no free oligomer DNA strand (lane 1) as covalent crosslinks are typically resistant to denaturing. If the non-covalent linkages, like electrostatic bonding of DNA--protein were subjected to denaturing (lane 3), and were not resistant to denaturing, all DNA would show as a DNA only band. However the electrostatic DNA-protein bond remains resistant to denaturing (compare lanes 2 and 3).

This resistance to denaturing suggests that the conditions for denaturing are not harsh enough to break the hydrogen bonds.

If a crosslink had formed in the modified strand, it would show up in lane 12 (DNA-protein complex row, Figure 3.5) with a limited amount, or no, free oligomer strand (DNA only row). The denatured DNA + protein (lane 9) would revert to the DNA only lane and not resemble that of to the DNA + protein (lane 8). The DNA + protein + chromium samples (lane 12) would not be affected by denaturing conditions if the bond was covalent. Adding a denaturant, 8 M urea (Figure 3.5), to DNA + protein + chromium only slightly disrupts DNA-protein binding in the case of modified DNA. Adding heat (50˚C, 10 min) to denature DNA-protein bonds effectively removes the shift lane for those samples subjected to denaturing conditions (lanes 3, 6, 9, 12, Figure 3.6).

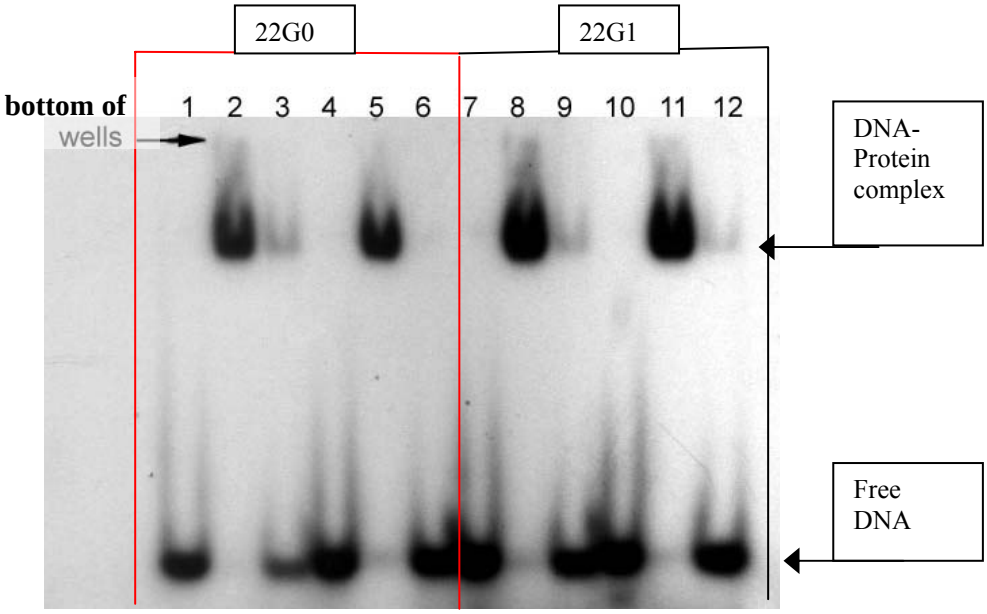

Figure 3.6: Gel comparison of control vs. 8-oxoguanine G1 DNA with and without chromium using heat and 8 M urea as a denaturant of p50BD and κB DNA on a 4% PAGE gel.
Lanes 1-6 unmodified DNA, Lanes 7-12 8-oxo G1 DNA
L→R the samples are DNA, DNA + protein, DNA + protein with urea, DNA + chromium, DNA + protein + chromium, and DNA + protein + chromium with urea.
*Denaturant (8M urea) in lanes 3, 6, 9, and 12

In Figure 3.6, the samples are in the same order as Figure 3.5. The chromium-free control sample (22G0 + p50BD) appears to be more resistant to heat and urea for the non-modified DNA, when comparing DNA bound to p50BD under denaturing conditions (lane 3) versus DNA bound to p50BD with chromium under denaturing conditions (lane 6). However, for modified DNA, urea (8 M) appears to affect DNA bound to p50BD subjected to denaturing conditions with and without chromium (lane 9 versus lane 12) similarly. The denaturing conditions are perhaps too harsh for unmodified DNA and DNA 8-oxoguanine modified at position 1 as the denatured hydrogen bonds (lanes 3, 9) are not distinctly different than their respective denatured chromium treated DNA-protein bonds (lanes 6, 12). It appears that the arrow indicating the DNA-protein complex row for sample 12 is very similar to the DNA-protein complex row for sample 9 which does not clearly indicate a DNA-protein crosslinking by chromium.

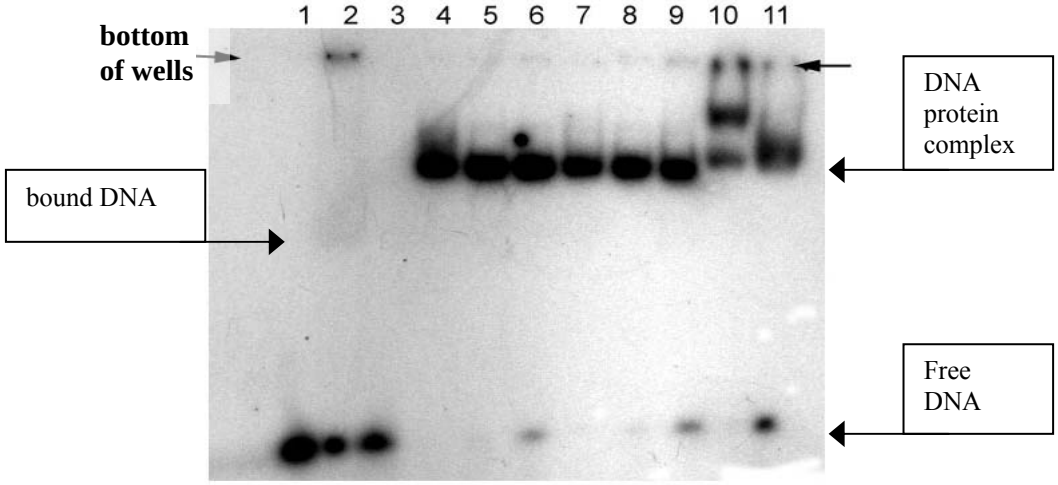

Figure 3.7: Gel of 8-oxoguanine G2 DNA with and without chromium using 8 M urea as a denaturant of p50BD and κB DNA.
Lanes 1-3: DNA (0.26 μM), DNA + hOGG1 + $NaCNBH_3$, DNA + chromium(V)-Salen
Lanes 4-9: DNA + p50BD (800 ng) + chromium(V)-Salen (0, 0.26, 0.52, 1.3, 2.6, 26 μM) + Urea
Lanes 10-11: DNA + p50BD + $NaCNBH_3$, DNA + p50BD + chromium + $NaCNBH_3$
On a 6 % DNA retardation gel

Figure 3.7 shows 8-oxoguanine modified at position G2 in κB DNA sequence bound with protein subjected to chromium oxidation. Lane 1 is a control lane to determine where unbound modified DNA travels on the gel. Lane 2 is the modified DNA bound to hOGG1 (by borohydride trapping, see the arrow indicating bound DNA, Figure 3.7). The hOGG1 enzyme has N-glycosylase and AP-lyase activity.[8] The hOGG1 enzyme can be reductively trapped on DNA with addition of $NaCNBH_3$ through the reduction of the Schiff base intermediate formed from lysine 44.[9,10] The use of reductively-trapped DNA—protein is a tool to determine if oxidatively-trapped DNA—protein (crosslinks) can be visualized on this type of gel. Due to the higher percentage of acrylamide for the gel in Figure 3.7 (6 %), a small amount of the radiolabeled DNA-protein treated with chromium or $NaCNBH_3$ stayed in the wells (lanes 4-11). Unlike the samples injected into the HPLC, the chromium was not removed from the samples before running the gel and has a tendency to block DNA-protein migration into the gel. In Figure 3.7, lane 3 is a control lane with DNA oxidized by chromium. Lanes 4 through 9 show DNA bound to p50BD protein subjected to increasing amounts of chromium. There is no discernable crosslink which would result in a shift visible on the gel. Lane 10, with DNA, p50BD protein, and using $NaCNBH_3$ as a reductant, gives a higher molecular weight complex than the DNA-p50BD + Cr(V)-Salen band (lanes 4-9). It is proposed that this corresponds to the formation of a p50BD homodimer bound to the κB DNA sequence as seen in Figure 2.11, page 39. Lane 11, where DNA is bound to protein, exposed to chromium, and subjected to $NaCNBH_3$ reductant for crosslinking, shows that the monomeric protein binding to DNA is restored (versus lane 10).

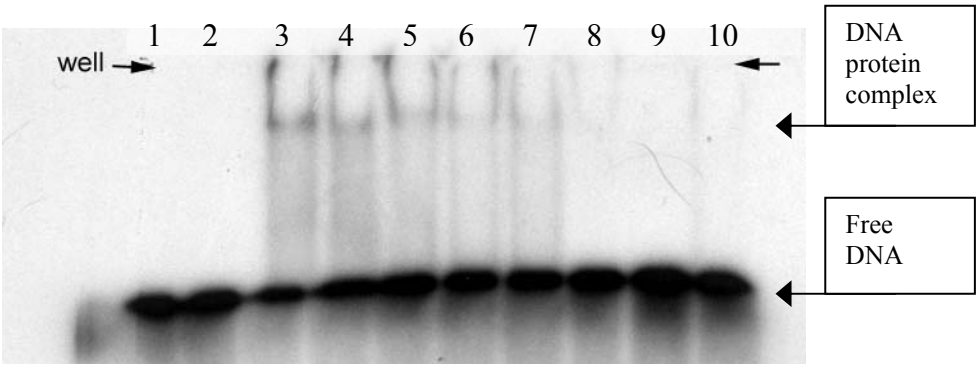

Figure 3.8: Gel of 8-oxoguanine G3 DNA with and without chromium using 8M urea and heat as a denaturant of p50BD and κB DNA
Lanes 1-2: DNA (0.26 μM), DNA + chromium(V)-Salen,
Lanes 3-4: DNA + p50BD (2500 ng), DNA + p50BD denatured (urea)
Lane 5: DNA + p50BD + chromium(V)-Salen,
Lane 6: DNA + p50BD + chromium(V)-Salen + urea,
Lane 7: DNA + p50BD + chromium(V)-Salen + urea (30 minute exposure),
Lane 8-9: DNA + p50BD + chromium(V)-Salen + 30˚C 5 min, Same with 60˚ C 5 min
Lane 10: DNA + p50BD + chromium(V)-Salen + urea + 30˚ C heat.
On a 4% urea gel

The p50BD protein has been shown to have poor binding to κB DNA when 8-oxoguanine modifies position 3 (see Figure 2.12, page 40). Figure 3.8 shows the binding of this G3 modified κB DNA (22G3) with p50BD, exposed to chromium and denaturing conditions. DNA bound to protein binds almost the same whether it is subjected to 8 M urea denaturing conditions (lane 4) or not (lane 3). Adding chromium and urea to the DNA-protein binding has little impact (lanes 5-7). However adding heat as a denaturant to the DNA-protein binding has great impact; even a gentle heat, 30˚C, completely abolishes any binding (lane 8). This is consistent with the overall weaker binding of p50BD to DNA 8-oxoguanine modified at this position.

Discussion

The samples run on the HPLC to detect DNA-protein crosslinking did not confirm or refute the presence of crosslinking. What was seen in Figure 3.4 was that the HPLC traces containing DNA with and without p50BD protein and chromium were similar. The two traces of DNA and chromium, one with and one without p50BD protein were similar, probably due to the ratio of DNA to chromium (1:1). It was thought that the ratio of 1:1 would be sufficient to see a difference between the samples. A higher amount of chromium to DNA would improve the resolution of the Gh/Ia and Sp peaks as seen in Figure 3.3. Earlier HPLC traces agreed with previous work that the p50BD protein shielded the DNA from the oxidative effects of chromium (data not shown). Nonetheless, a peak for the 8-oxoguanine DNA was determined to have eluted at the same time for all traces (8.4 minutes). Parts of the solution, including any residual buffer salt from the cation exchange column, elute quickly. Specifically, these peaks were seen at 1.5 to 2.5 minutes.

It is possible that there was not enough protein to successfully bind the κB DNA or that running the DNA-p50BD protein complex through the cation exchange column disrupted some protein hydrogen bonds. The amount used was sufficient to cause a 100% DNA shift. Gel systems with 5'-^{32}P radiolabeled double-stranded DNA can use a much smaller amount of DNA to visualize interactions and there is no cation exchange column requirement. On the HPLC, a small amount of protein will certainly bind the DNA, yet an insufficient amount of protein might not clearly show the DNA-protein complex shifted to a different retention time. This four-sample HPLC determination of DNA-protein crosslinking was run earlier using a solution buffer with DTT and a higher

ratio of chromium to DNA (1000:1) where the shielding effects of the protein were visible by HPLC trace (data not shown). Figure 3.4 had no DTT in the sample preparation; this last HPLC trace assumed that the DTT of 2.5 mM reduced the chromium(V)-Salen (0.5 mM). It was determined that the HPLC separation based on charge was not the correct system for visualizing DNA-protein crosslinks.

Modified 22-mer DNA and p50BD protein together are quite sizable (13.5KDa and 42.4 KDa respectively) which can be a problem when using an older HPLC column. Charge separation was not conclusive; thus a gel system was a better choice to determine covalent crosslinking for whole protein—DNA. The benefits include a smaller concentration of DNA can be radiolabeled with ^{32}P-γ-ATP and still be visualized, and there is no cation exchange column DNA loss as there is no clean-up required to remove excess chromium for samples run on a gel.

For Figure 3.5, for unmodified DNA, lanes 1-6, the gel implies that chromium oxidation could cause covalent crosslinking, but more harsh denaturing conditions are required to prove the crosslinking. The non-modified DNA bound to protein and subjected to chromium and denaturing conditions (lane 6) appears *more resistant* to denaturing than DNA bound to protein and subjected to denaturing conditions (lane 3) as determined by the amount of unbound DNA (see free DNA arrow). This result does support the theory that a covalent bond is more resistant to degradation than an electrostatic bond for DNA-protein crosslinking.

In Figure 3.5, for 8-oxoguanine modified at position G1 DNA implies that the bond is not covalent when bound to p50BD protein and exposed to chromium. It seems that DNA–protein subjected to chromium and denaturing conditions (lane 12) appears

less resistant to denaturing to denaturing than DNA bound to protein and subjected to denaturing conditions (lane 9). This implies that there was no covalent linkage of modified DNA with p50BD protein and that the chromium was able to oxidize either the DNA or the protein and decrease the electrostatic bonding of the DNA and protein as evidenced by unbound DNA (see arrow 'free DNA' Figure 3.5). The DNA bound to protein subjected to denaturing 8 M urea (lane 9) is *less* degraded than the sample of DNA bound to protein not subjected to 8 M urea (lane 8) which indicates an unusual relationship of urea with modified κB DNA and the truncated p50 protein. It is known that the κB DNA is close to B-form DNA and that when the p50 protein binds to it, there is only a slight unwinding in the 5'-GGGG-3' area and a very small bend produced in the DNA. It is possible that the 8-oxoguanine with p50BD protein bound is structurally perturbed compared with unmodified κB DNA with p50BD bound, and adding urea to the system disrupts non-specific protein binding, permitting the DNA to adopt a more B-form shape, which allows for the protein to bind tighter to the DNA. The bound DNA-protein complex bands remaining for the urea treated lanes, 3, 6, 9, and 12 suggests that the denaturing conditions are not strong enough to break hydrogen bonds.

Increasing the denaturing by using mild heat had a drastic effect on the denatured samples (Figure 3.6). For the unmodified DNA, it appeared that DNA bound to protein exposed to chromium (lanes 6) was denatured more than the DNA bound to protein (lanes 3), in direct contrast to what was seen in Figure 3.5. For 8-oxoguanine modified DNA, the effects of denaturing the DNA-protein complexes with and without chromium exposure were essentially the same (lanes 9 compared to 12) which was slightly different from the pattern seen in Figure 3.5. The 8-oxoguanine G1 DNA incubated with protein

and exposed to chromium and urea/heat had similar amounts of residual binding as well as free (non-protein bound) DNA as the modified DNA incubated with protein and exposed to urea/heat. It is possible that the tighter binding affinity of control DNA, 0.605 μM, compared to the binding affinity for 8-oxoguanine modified at position G1 DNA, 1.849 μM, with p50BD protein contributed to the variation of the effects of heat/urea on the different κB DNA sequence (see table 2.6, page 49).

For κB DNA 8-oxoguanine modified at position G2 bound to p50BD protein subjected to chromium oxidation (Figure 3.7), increasing amounts of chromium does not appear to covalently link the DNA and the protein. In lane 10, DNA bound to protein and exposed to sodium cyanoborohydride gives the dual banding pattern proposed to be the p50BD homodimer seen in the EMSA, Figure 2.11, page 39. It is possible that the $NaCNBH_3$ reduced some of the p50BD protein strand and altered the binding of the monomeric protein to DNA. The sample 'DNA + p50BD + chromium + $NaCNBH_3$' mimicked the binding of the DNA-protein bands. It was seen earlier that as the amount of p50BD protein increased past a certain concentration of protein (2.356 μM), the p50BD began to bind as a proposed dimer. This could indicate that at higher amounts of truncated p50 protein allosteric cooperative binding is possible. Without a crystal structure of the truncated form of the p50 protein, it is difficult to determine the exact effects of truncating the protein. It is possible that the amino acid residues not included stabilized the full p50 protein at the dimerization interface, which is in the C-terminal domain and has six variable loops.

When using κB DNA 8-oxoguanine modified at position G3, it was seen that chromium and urea have little impact on binding of DNA and p50BD protein (Figure 3.9,

lanes 4-7). The binding of the p50 was poor, regardless of any sample additions such as chromium and urea. Adding heat as a denaturant was detrimental to binding; all samples subjected to heat had no protein bound lane (Figure 3.9, lanes 8-10), as expected.

Taken together, these results indicate that no apparent covalent crosslinking occurs with unmodified κB DNA and p50BD protein when subjected to chromium as an oxidant. Furthermore, the above results indicate that 8-oxoguanine-modified at positions G1 through G4 κB DNA sequences also do not covalently crosslink to p50BD protein.

[1] Berman, H.M., Westbrook, J., Fangs, Z., Gilliland, G., Bhat, T.N., Weissig, H., Shindyalov, I.N., Bourne, P.E. (2000) The Protein Data Bank. *Nucleic Acids Res.* **28**, 235-242.

[2] Huang, B.-D., Vu, D., Cassiday, L.A., Zimmerman, J.M., Maher, L.J., and Ghosh, G. (2003) Crystal structure of NF-κB $(p50)_2$ complexed to a high-affinity RNA aptamer. *Proc. Natl. Acad. Sci. USA* **100**(16), 9268-9273.

[3] PDB ID: 1SVC.

Müller, C.W., Rey, F.A., Sodeoka, M., Verdine, G.L., and Harrison, S.C. (1995) Structure of the NF-κB p50 homodimer bound to DNA. *Nature* **373**, 311-317.

[4] Voet, D. and Voet, J.G. Biochemistry, 2nd Edition. 1995, New York: John Wiley & Sons, Inc.

[5] US Patent 6,309,673, http://www.pharmcast.com/Patents/Yr2001/Oct2001/103001/6309673_Dialysis103001.htm

[6] Sugden, K.D., Campo, C.K., and Martin, B.D. (2001) Direct oxidation of guanine and 7,8-dihydro-8-oxoguanine in DNA by a high-valent chromium complex: a possible mechanism for chromate genotoxicity. *Chem. Res. Toxicol.* **14**, 1315-1322.

[7] Hailer-Morrison, M.K., Kotler, J.M., Martin, B.D., and Sugden, K.D. (2003) Oxidized guanine lesions as modulators of gene transcription. Altered p50 binding affinity and repair shielding by 7,8-dihydro-8-oxo-2'-deoxyguanosine lesions in the NF-κB promoter element. *Biochemistry* **42**, 9761-9770.

[8] Bjørås, M., Luna, L., Johnsen, B., Hoff, E., Haug, T., Rognes, T., and Seeberg, E. (1997) Opposite base-dependent reactions of a human base excision repair enzyme on

DNA containing 7,8-dihydro-8-oxoguanine and abasic sites. *EMBO J.* **16**(20), 6314-6322.

[9] Fromme, J.C., Burner, S.D., Yang, W., Karplus, M., Verdine, G.L. (2003) Product-assisted catalysis in base-excision DNA repair. *Nat. Struct. Biol.* **10**(3), 204-211.

[10] Slade, P.G., Hailer, M.K., Martin, B.D., Sugden, K.D. (2005) Guanine-specific oxidation of double-stranded DNA by Cr(VI) and ascorbic acid forms spiroiminodihydantoin and 8-oxo-2'-deoxyguanosine. *Chem. Res. Toxicol.* **18**(7), 1140-1149.